Postharvest Biology and Technology 211 (2024) 112722

Contents lists available at ScienceDirect

Postharvest Biology and Technology

journal homepage: www.elsevier.com/locate/postharvbio

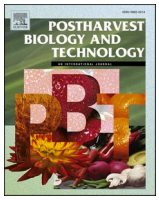

The virtual container: Physics-based simulation of refrigerated container map temperature and fruit quality evolution and variability in a shipment

Thijs Defraeye [a,b,*], Celine Verreydt [a,b], Julien Gonthier [a], Leo Lukasse [c], Paul Cronjé [d,e], Tarl Berry [d,e]

[a] Empa, Swiss Federal Laboratories for Materials Science and Technology, Laboratory for Biomimetic Membranes and Textiles, Lerchenfeldstrasse 5, CH-9014 St. Gallen, Switzerland
[b] Food Quality and Design, Wageningen University & Research, P.O. Box 17, 6700 AA Wageningen, the Netherlands
[c] Wageningen University and Research, Bornse Weilanden 9, 6708 WG Wageningen, the Netherlands
[d] Citrus Research International, Nelspruit, South Africa
[e] Department of Horticultural Science, Stellenbosch University, Stellenbosch, South Africa

ARTICLE INFO

Keywords:
Multiphysics
Computational
Citrus
Digital twin
Refrigeration: slot-ventilated enclosure

ABSTRACT

Many fresh food and vegetables are transported in refrigerated containers after harvest, often over thousands of kilometers. A better understanding of when and where food quality is lost in these supply chains provides opportunities to reduce the quality variability within and between different shipments. Nowadays, however, only a few (hygro-)thermal sensors are placed within every shipment, which masks the variability in the shipment. These hygrothermal data are also not actionable for stakeholders for decision-making. The resulting food quality evolution and its variability within a shipment remain invisible. We approach this problem by building a validated physics-based digital model of a refrigerated container for citrus fruit. This virtual container model is described extensively in an accompanying paper (Defraeye et al., 2024). We use computational fluid dynamics with a two-phase porous media approach to simulate the airflow in this virtual container. We also simulate the cooling process of every single fruit and the fruit's thermal quality loss. We compare the virtual container model with a full-scale experimental data set. The simulations captured the main physical trends of container cooling but cooled on average 0.3 d faster. The variability in seven-eighths cooling time within the cargo was over 2 days, and that of the remaining shelf life after the transport period of 24 days was about 0.7 days. We identify the slowest cooling location in the cargo. This location is the pallet or box that would need to be inspected to assess the quality or the best location to place the sensors. The model simulations indicate that during the container's warm loading or hot stuffing, high airflow rates should be used for the first three days to improve fruit quality preservation. Lower airflow rates can be used later on. The simulations show that airflow bypasses through gaps between pallets should be avoided. Using a void plug can decrease the cooling time by 30%. Void plug placement is found to be much more effective than reducing the small gaps between the pallets. The type of void plug that is used is less critical. Cooling and quality problems could be mitigated by placing precooled pallets at the expected slowest cooling locations in the container. Changing the T-bar floor height, while keeping the pallet height constant, affected the differences in cooling and quality between both sides of the container. The virtual container provides a full spatiotemporal map of the fruit temperature, temperature-driven quality, and postharvest life for all fruit in the container. We quantified cooling times and remaining shelf life in 60,000 individual probe locations. The data that are engineered by the virtual container is currently a missing link to enable in-transit temperature management, shelf-life-driven logistics, and inventory management. The virtual container is also an essential building block of a refrigerated container's digital twin that can help reduce food loss and increase supply-chain resilience. Such simulation tools will support stakeholders in the future in evaluating and improving cargo temperature control and resulting fruit quality at arrival.

* Corresponding author at: Empa, Swiss Federal Laboratories for Materials Science and Technology, Laboratory for Biomimetic Membranes and Textiles, Lerchenfeldstrasse 5, CH-9014 St. Gallen, Switzerland.
E-mail address: thijs.defraeye@empa.ch (T. Defraeye).

https://doi.org/10.1016/j.postharvbio.2023.112722
Received 17 July 2023; Received in revised form 24 October 2023; Accepted 5 December 2023
Available online 15 February 2024

1. Introduction

Many fresh food and vegetables are transported at increasingly larger volumes in refrigerated containers after harvest, often over thousands of kilometers. In 2019, 3.1 million refrigerated twenty-foot equivalent units (TEU) were in operation, which is expected to double by 2030–6.0 million TUE (Prescient & Strategic Intelligence Private Limited, 2021). This increase is driven by the larger amount of food that needs to be produced, often counter-seasonally, to feed the worldwide population, the increasing demand for pharmaceutical drugs, the rising amount of trade routes, the availability of technology for real-time tracking, and expanding e-commerce (Prescient & Strategic Intelligence Private Limited, 2021). Reduced food losses after harvest on the farm will also enable stakeholders to access more distant markets (Carrier, 2020). Refrigerated containers are required to enable these exports. Refrigerated containers are also used as remote and flexible cooling units in locations where other cooling or precooling facilities are unavailable (Defraeye et al., 2016a, 2015b). In addition, an upcoming trend is the use of 45-foot railway-refrigerated containers to transport on-land over large distances, for example, to help support the 'new silk road' (Zhao et al., 2018).

Despite the large number of refrigerated containers, several problems remain unsolved concerning maintaining the cargo at an optimal storage temperature (Hamburd-Sud, 2021). Airflow short-circuiting occurs via gaps between the pallets and the walls or at the back of the container. A part of the cold air bypasses the pallets and is not used to cool the cargo. Also, the cooling of the cargo is not uniform, as some locations cool less than others (Defraeye et al., 2016b). Even hot spots, which are significantly warmer pockets, occur due to insufficient ventilation, respiratory heat production, or both (Jedermann et al., 2017, 2014). On the other hand, fruit exposed to the cold delivery air temperature at the bottom of the container can develop chilling injury (Defraeye et al., 2016b; Shrivastava et al., 2022). Also, the airflow distribution in the container largely depends on the packaging and pallet loading pattern. These issues make the cooling and fruit quality evolution during refrigerated transport suboptimal. When we better understand when and where food quality is lost in these supply chains, we can reduce the quality variability within and between different shipments and help reduce food loss.

Nowadays, stakeholders intensify in-transit hygrothermal monitoring of the environmental conditions to which the cargo is exposed and thereby gather more food data at every gateway along the supply chain (Jedermann et al., 2017; Khumalo et al., 2021; Mercier et al., 2017; Ndraha et al., 2018). However, only a few (hygro-)thermal sensors are placed within a commercial shipment (Chaomuang et al., 2021; Defraeye et al., 2021; Jedermann et al., 2014; Mercier et al., 2017; Shoji et al., 2022). The main reasons are sensor cost, the additional workload of placing and retrieving the sensors, and the time and expertise required to analyze the data. As a result, the variability in cooling between individual fruit or vegetables in the shipment is masked, although present in several studies. Finally, the sensors measure the air temperature (and humidity), which often differs from what the fruit pulp is exposed to. The food quality evolution and its variability within a shipment remain invisible. This lack of insights limits the potential benefits of new container management strategies such as remote container management (RCM). With RCM, the environmental conditions in the container can be altered remotely in real-time to improve the quality preservation of the cargo. However, we currently lack actionable data on the cargo to make an informed decision on how to change the container refrigeration unit's set points. Another bottleneck is that the installed sensor data systems that monitor the cargo are now disconnected from the RCM system and often deploy different software platforms (Jedermann et al., 2017). In addition to the hygrothermal data, we would also need data on the products' remaining postharvest quality, for example.

Researchers have mapped the temperature and food quality evolution and variability in containers with full-scale experiments (Berry et al., 2021; Chaomuang et al., 2021; Defraeye et al., 2016b; Getahun et al., 2017; Jiang et al., 2020; Merai et al., 2019; Mercier et al., 2017). Typically, such experiments are performed on commercial shipments. The reason is that the fruit needed to fill the container often has a market value of several 10,000 USD. Experiments on a full container are very expensive, given the risk of partial loss. Filling the container with fruit simulators, such as water-filled spheres, enables one to do many repetitions with the same products but is also very labor-intensive to set up. Furthermore, lab-scale experiments take days to cool down the cargo due to the slow cooling process. Given the high workload and limited accessibility in commercial supply chains, full-scale experiments are only sporadically performed. For that reason, researchers and industry have reached out to physics-based simulations based on computational fluid dynamics (Mercier et al., 2017). Modelers aim to evaluate different scenarios rapidly in-silico, i.e. experiments performed by means of a computer, and to obtain complementary data. Typical applications are to identify how to optimize airflow in a container, evaluate container stowing strategies, evaluate ventilated packaging, or identify hot spots (Berry et al., 2016; W. Wu et al., 2019a; Wu et al., 2018). The main bottlenecks are that (1) only airflow and cooling are typically looked at, and food quality is not considered, (2) often fruit and air are modeled as a single phase during cooling, which assumes that they are perfectly mixed, (3) most in-silico research focuses on refrigerated trucks and trailers, and few research groups study refrigerated containers, (4) several research questions have been left unanswered, for example, the impact on fruit quality evolution and the heterogeneity within the cargo of following parameters: gaps between the pallets, void plug types, the airflow rate at the inlet and the T-bar floor height, among others.

In this study, we aim to tackle these knowledge gaps. On the one hand, we aim to advance our understanding of cooling and food quality evolution and variability in a refrigerated container and, on the other hand, to advance the physics-based modeling of refrigerated enclosures. To this end, we build and validate a physics-based virtual container for citrus fruit shipped from South Africa to Europe. We focus on the ambient loading or hot stuffing process, which implies that cargo is loaded warm to mitigate the shortage of cooling facilities. Ambient loading is often used for citrus (Defraeye et al., 2015b) and is standard practice in banana fruit (Jedermann et al., 2017). Both are packed in ventilated packaging, but bananas are typically packed in a plastic liner. Although fast precooling of the fruit after harvest is preferred for optimal quality preservation, ambient loading is sometimes used in the industry. One reason is that the precooling facilities, which have limited throughput, are overloaded during the peak harvest season in some countries. Then, containers are used as mobile precoolers. In addition, ambient loading enables to cool in transit and thereby saves time in handling, for example in the banana industry. Smallholder farmers also use such units for cooling their produce at the farm, because they lack access to precoolers. Although this is a less optimal solution as containers cool much slower than commercial precoolers, it is typically better than leaving the produce uncooled. We use computational fluid dynamics (CFD) with a two-phase porous media approach to simulate the airflow in the container and through the ventilated packaging. We can thereby monitor the cooling process of every single fruit in the shipment. We also simulate the fruit's thermal quality loss. This virtual container thus mimics in-silico the aging of the full cargo. With this virtual container, we investigate the impacts of various airflow rates, gaps between the pallets, void plug strategies, partial precooling of the cargo, and adjusting the height of the T-bar floor.

2. Materials and methods

2.1. Physics-based model and simulation

The full description of the computational model of the virtual container is presented in detail in an accompanying paper (Defraeye

et al., 2024). There we present the (1) geometrical model of the container; (2) governing equations for airflow and heat transfer in air and in the porous medium (ventilated packaging); (3) governing equations for the evolution of fruit quality attributes; (4) boundary and initial conditions; (5) spatial and temporal discretization; (6) numerical simulation; (7) the metrics that we use for evaluating cooling and food quality; (8) the verification and validation experiments. Therefore, only the main model features are highlighted below.

We developed a 2D continuum, finite-element model of a 40-foot refrigerated container hold (Fig. 1). This model includes the inlet section, a baffle plate at the refrigerator unit side, the narrow open space of channels within the T-bar floor, the openings in the T-bar floor, the open space between the wooden pallets' base and the pallet's top wooden slats, the top slats of the wooden pallets, the palletized fruit, the small vertical gaps between the pallets, and the return air duct. Note that only the top slats of the wooden pallet were accounted for, as these will have the highest impact on the airflow. The wooden connectors between the bottom and top of the pallet base and the bottom slats of the pallet were not modeled. Also note that there are gaps on the pallets' lateral sides, between the pallets themselves at the centerline, and between the pallet and the vertical container walls. These could not be explicitly accounted for in the present model.

The 2D model was developed so that it is equivalent to the 3D container as much as possible. We do not model the refrigeration unit itself. The container holds 20 pallets of 16.5 kg ventilated carton boxes filled with 102,400 'Navel' oranges. The fruit is loaded into the container at an ambient temperature of 16 °C. The fruit are cooled by vertical airflow from bottom to top at 2 °C and 4150 $m^3\,h^{-1}$ for 24 days, simulating a shipment from South Africa to Europe. We model airflow and convective heat transfer in the container with CFD using the Navier-Stokes equations in combination with the k-ε turbulence model. We model turbulent airflow in the ventilated cargo using the Darcy-Forchheimer equation in porous media. We model the cargo's convective and conductive heat transfer using a two-phase porous medium approach. We can thereby monitor the cooling process of every single fruit in the shipment. We model the evolution of the fruit quality index with a kinetic-rate-law model. The kinetic rate law model quantifies the change of the fruit quality index, and was modeled as a function of temperature and time after cooling. The remaining shelf life can be predicted based on the remaining quality at the end of the supply chain and the quality where the food is considered to be lost. The remaining shelf life can be predicted by taking the known final quality at the end of the supply chain, prior to shelf life storage, and by keeping the fruit as of that point in time at constant conditions until the threshold is reached. More details can be found in (Defraeye et al., 2024).

Other quality attributes relevant to citrus (Shrivastava et al., 2022) are not modeled in this study, such as chilling injury, pest mortality, and mass loss. All models implemented in the container model are calibrated or validated with experimental data. We also compare the computed fruit temperatures inside the container with a full-scale experiment. The physics-based model is implemented in COMSOL Multiphysics (version 6.1). COMSOL is a finite element-based commercial software. A sensitivity analysis verified the spatial and temporal discretization. Transient simulations are run with a time step below 600 s

The actionable metrics that are extracted from the simulation are: (1) the seven-eighths cooling time (SECT) of the fruit at each location in the cargo [h]; (2) the index of remaining postharvest fruit quality [%], (3) the associated remaining shelf life [d]. Note that the SECT is used here to quantify the cooling behavior of the fruit. Although the SECT is frequently used in commercial (pre)cooling operations, note that the fruit temperature has not yet reached the required storage temperature. We used it in this study to quantify differences between cooling scenarios.

2.2. Simulated cases

The base case simulates the cooling of the refrigerated container and its cargo starting at 16 °C, at a constant delivery air temperature (DAT), also called supply air temperature (SAT), of 2 °C and a constant airflow rate for 24 days at 4150 $m^3\,h^{-1}$. These conditions are representative of overseas citrus transport from South Africa to Europe. These conditions were determined from air temperature measurements in several commercial shipments from South Africa to Europe. Afterward, the fruit is held at ambient conditions, with a DAT of 23 °C, to mimic shelf-life conditions at the retailer.

In addition to the base case, various cold chain cases were simulated (Table 1), by varying the operational conditions and cargo-container parameters, compared with those of the base case:

1. We evaluate the impact of various airflow rates since a container can run at two airflow regimes.
2. We analyze the impact of the gaps between the pallets
3. We evaluate the impact of different void plug strategies. A void plug is a blockage structure that is installed at the door end of the refrigerated container, at the bottom of the last pallets, to reduce flow bypass via this open space. The void plug material is typically a tarp or cardboard material.
4. We analyze if the container's slowest cooling location can be mitigated by loading a few pallets that are precooled at these critical locations.
5. We analyze if adjusting the height of the T-bar floor leads to an improvement in the cooling uniformity in the container.

The base case corresponds to the normal void plug variant (L-shaped at the bottom) and a gap of 20 mm between the pallets. Note that a shorter time frame was simulated for some of these simulations, namely 5 days. The reason is that the cooling down process takes place in the first 2–3 days. After the cargo is cooled down, the differences in thermal aging between the fruit in the shipment are present (3.2.2) but less pronounced as they are kept at the same temperature.

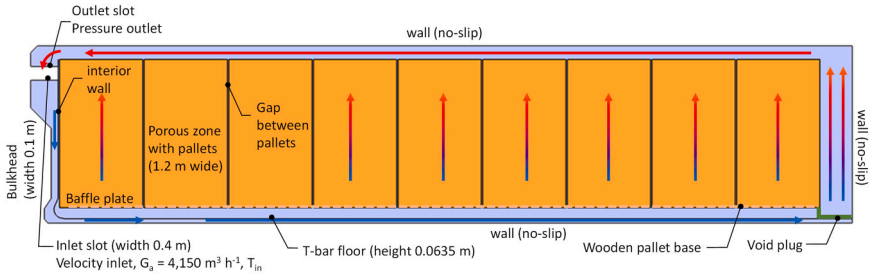

Fig. 1. Computational model and boundary conditions. The blue arrows indicate cold airflow and red arrows indicate warm airflow, as air heats up when cooling down the fruit.

Table 1
Cooling process conditions used for the different simulations (a dash indicates the same conditions as the base case are used).

Name	Case	Initial fruit temperature	Delivery air temperature (DAT)	Speed or airflow rate	Duration
Base case (24 days transport)	Refrigerated container, warm loaded	T_{fr} = 16 °C	T_{DAT} = 2 °C	4150 $m^3\ h^{-1}$	24 days
Base case (5 days)		-	-	-	5 days
Comparison full scale experiment	-	-	Variable temperature-time data from experiment	-	5 days
High & low airflow rates	-	-	-	1038 $m^3\ h^{-1}$ (25%), 2075 $m^3\ h^{-1}$ (50%), 4150 $m^3\ h^{-1}$ (100%), 6225 $m^3\ h^{-1}$ (150%)	5 days
Gaps	5 gap sizes: 0 mm, 10 mm, 20 mm (base case), 40 mm, 60 mm	-	-	-	5 days
Void plug strategies	5 void plug variants	-	-	-	5 days
Partially precooling the cargo	Few pallets precooled to 4 °C prior to loading of the pallets	-	-	-	5 days
Height T-bar floor adjusted	Floor adjusted to 127 mm, 111, 95, 79, 50.8, 42.3 mm instead of 63.5 mm	-	-	-	5 days

3. Results and discussion

3.1. Comparison with full-scale experiment for ambient loading

3.1.1. AIM

We compare the cooling behavior of a simulated refrigerated container (base case) during ambient loading of citrus fruit with a full-scale experiment ((Defraeye et al., 2016b), see (Defraeye et al., 2024)). We aim to show that our simulations capture the cooling process with sufficient accuracy. The physics implemented in the model were validated in previous studies (Defraeye et al., 2019; Shrivastava et al., 2022). The porous medium model was validated in (Defraeye et al., 2024). Note that the set air temperature was here 1 °C.

3.1.2. Results

Fig. 2 shows the measured and simulated temperatures at the container outlet, so the return air temperature. In addition, the inlet temperature and the air temperature for the pallet at the door end of the container (indicated by the blue dot in Fig. 3) are shown. The latter location is where a commercial sensor is often placed since it is a location that is easy to reach and is the furthest away from the refrigeration unit. Fig. 3 shows the fruit core temperatures at different positions in the refrigerated container for experiments and simulations. The temperature differences between experiments and simulations are also shown. We only report the first 5 days of the experiment since the simulations and experiments agreed well afterward. The reason is that the cargo was cooled down in the first days of the experiment. Fig. 4 shows the half-cooling time for all sensor locations that is extracted from the cooling curves of Fig. 3.

Note that we expect the results to not exactly match due to the intrinsic differences between the simulations and experiments, which we briefly highlight. A key difference between the model and the experiment is the packaging type used and its stacking pattern on the pallet. In both simulations and experiments, Supervent packaging is used, but the number of vent holes on this package in the experimental study was reduced. The reason is that these packages provided better mechanical stability. Also, a staggered stacking of boxes on the pallet was used in the experiments to enhance mechanical stability, which led to the blocking of some of the vent holes. As a result, the airflow resistance in the experiments is expected to be slightly larger than in the simulations. In addition, the initial fruit temperature for the simulations was taken uniformly throughout the cargo. In the experiments, however, this temperature differed up to a few degrees Celsius, depending on the location. Given these differences, this report should not be considered a pure validation study but rather a quantitative comparison between experiments and simulations.

3.1.3. Conclusions

First, we can conclude that the simulations capture the main cooling trend of the experiment in the vertical direction, namely that the bottom

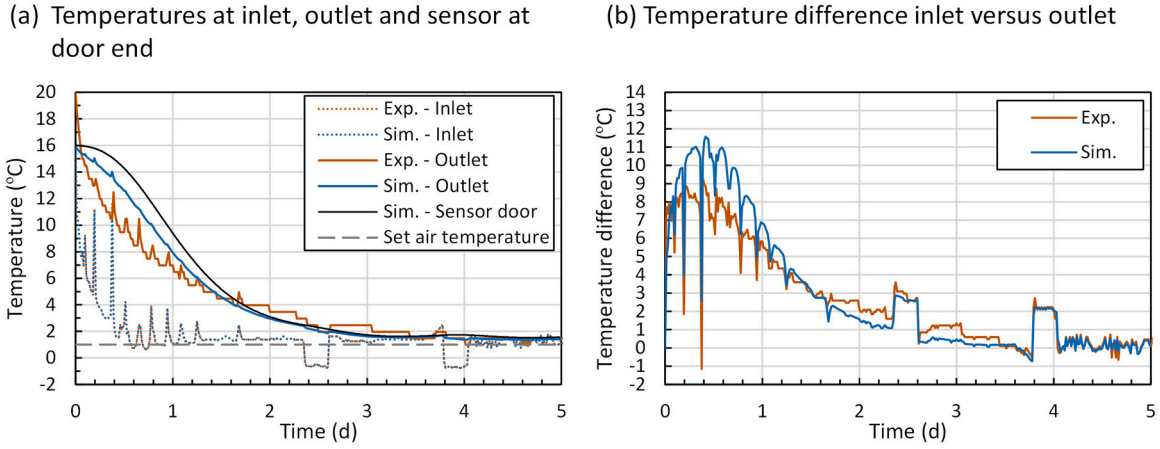

Fig. 2. Environmental conditions in the containers, as logged by the container's sensors in the experiments and from porous media simulations (a) temperature of supply and return air as well as a simulated temperature sensor on the last pallet at the door end a height of 2 m above the container floor; (b) temperature difference between supply and return air, which is representative for the difference in sensible heat that is removed from the cargo.

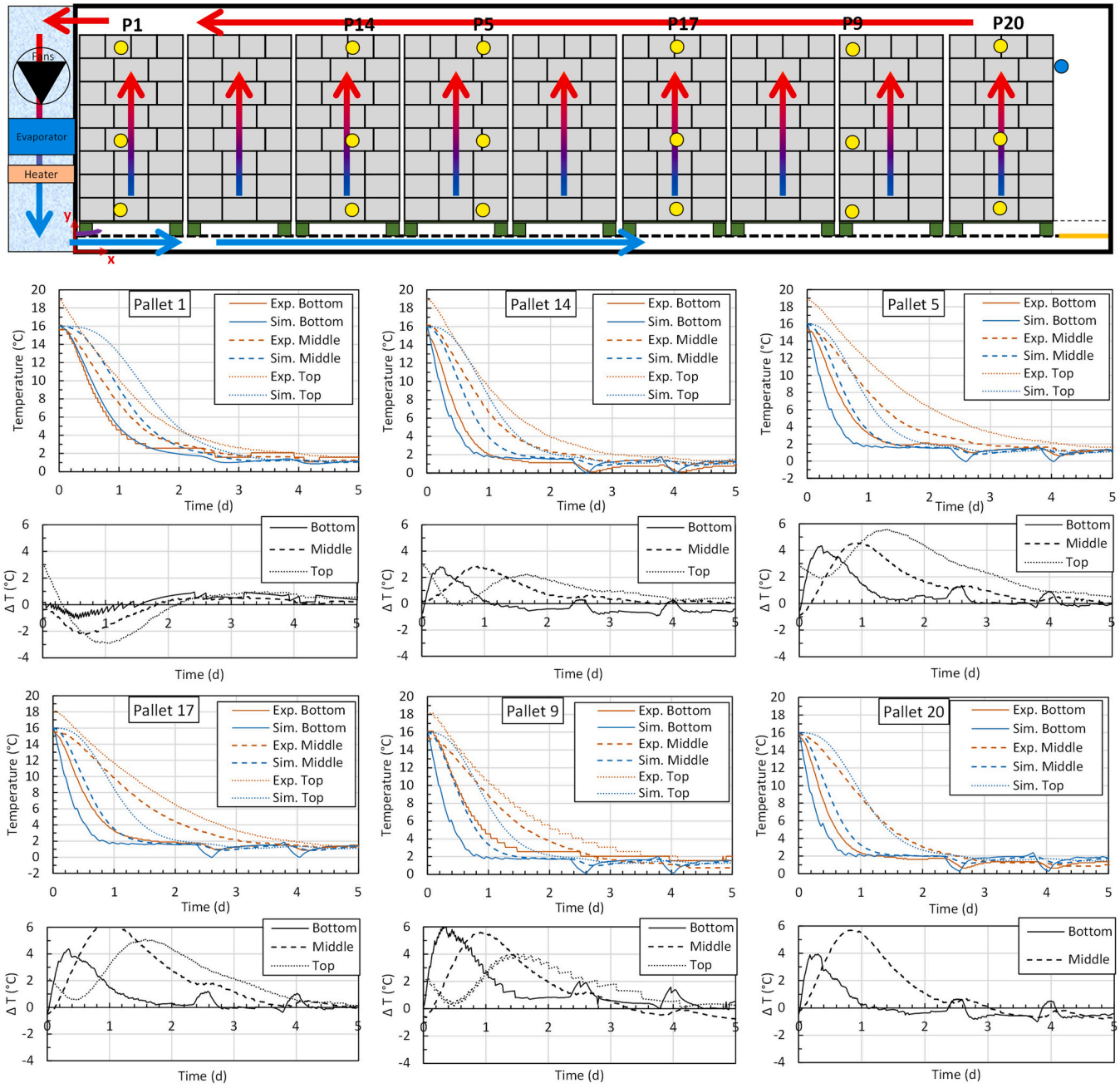

Fig. 3. Fruit core temperature in six pallets in the refrigerated container at three different heights in the pallets (P) from experiments and simulations. The location of the sensors is indicated with yellow dots on the container map. The temperature difference between experiments and simulations is also shown (ΔT). The blue dot indicates the location of the sensor at the door end in a side view of the container.

of the pallets cools faster than the middle and top. The simulations, however, predict the experimental cooling trend in the horizontal direction less accurately: experiments show a longer cooling time in the middle of the container (pallets 5, 17, and 9), whereas simulations predict a more uniform cooling in this region.

Second, the fruit in the simulations cools faster than in the experiments. The differences in the cooling curves are between 2 and 6 °C during the first days of cooling. The half-cooling time over all measuring points differs on average by 0.3 days, so 30%, between experiments and simulations. However, larger differences up to 0.65 days, so 70%, are found for several locations, which is substantial. Several reasons for these discrepancies exist, in addition to several model simplifications that have been made (see (Defraeye et al., 2024)). One possible reason could be the fact that a slightly different packaging type has been used in the experiments. Apart from affecting the fruit cooling inside the packaging, the packaging will also affect the pressure resistance the container fans must overcome. As a result, the resulting airflow rate that the fans deliver may differ between experiments and simulations. We do not know to which extent this effect plays a role on the results. In addition, the imperfect stacking of the boxes on the pallet and pallet placement in the real container will also affect the pressure resistance and the airflow field.

Third, the pallet close to the refrigerator unit (pallet 1) cools slower than in the experiments. The reason for this is likely that there is a recirculation zone at the bottom of this pallet that is predicted in-silico. This zone can trap the air to some extent and thereby reduce heat removal. A detailed description of this phenomenon can be found in (Defraeye et al., 2022).

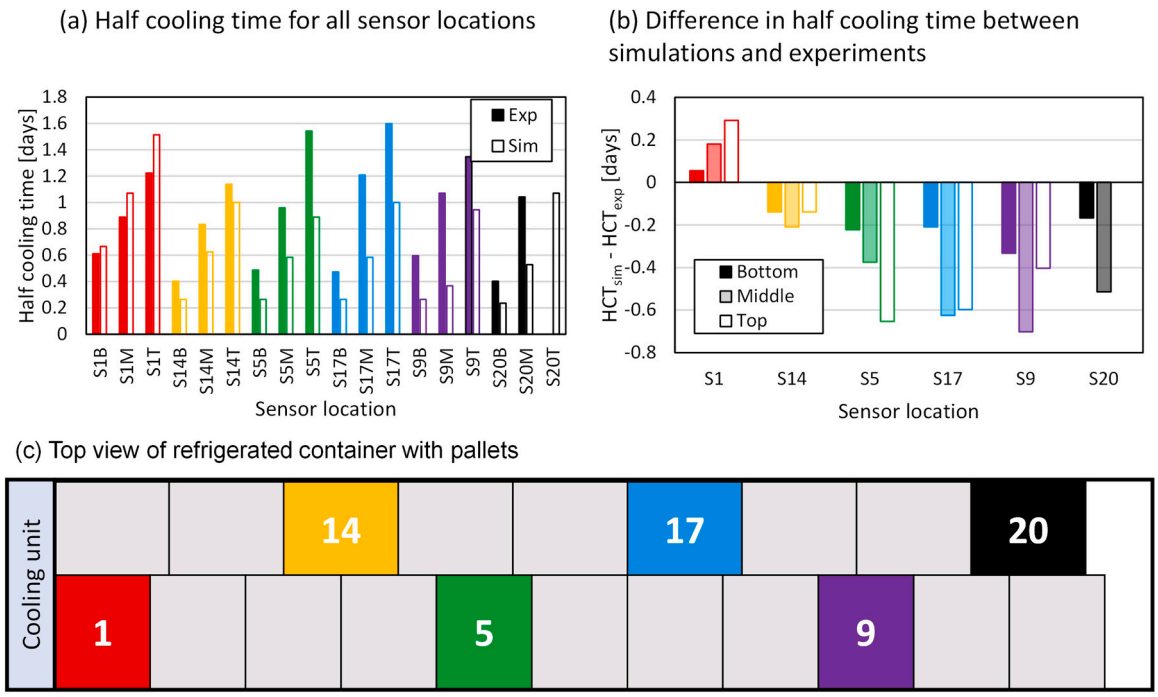

Fig. 4. (a) Half-cooling time (HCT) for all sensor locations. (b) The difference in half-cooling time between simulations and experiments split up per pallet. (c) Top view of the pallets with each monitored pallet in a different color.

Fourth, the simulated return air temperature decreases slower than in the experiments in the first 36 h. After that, an inflection point occurs where the heat removed from the experiments is lower than that of the simulations. This faster-simulated decrease implies that more sensible heat is removed from the cargo than in the experiments at the start. After about 48 h of cooling, both temperatures matched well.

Fifth, we analyze the air temperature sensor at the door end of the container. This air temperature sensor lies closer to the return air temperature than to the supply air temperature. In summary, the simulations accurately predict the physics of cooling, especially given all the sources of inherent differences with the experiments. The vertical gradients are predicted well, and the simulations predict a slightly faster cooling than in the experimental observations.

Finally, as we will show below (sections 3.4 and 3.5), the predicted cooling rate of the pallets in the container is, to a large extent, dependent on the amount of air that bypasses the cargo through the gaps between the pallets, the impact of the gaps between the pallets and the void at the door end. As such, differences in fruit cooling rates of our model versus experiments are likely caused partially by a different airflow rate through the pallets, in addition to different airflow distributions inside the container. We explored the solutions' sensitivity to different parameters in the supplementary material. Here we evaluated the impact of the T-bar floor height, the void plug, the gap between pallets, and laminar versus turbulent flow simulations.

However, we refrained from tuning the model parameters to obtain a better agreement with experiments, as this is not according to best practice in multiphysics modeling.

In previous research, a substantial discrepancy in cooling rates has been observed in experiments between seemingly identical containers (Berry et al., 2021). Although the containers appeared to be identical, minor variations in pallet shape (lean or tilt) or in the positioning of the loaded pallets contributed to significant differences in the gaps between the pallets. These small discrepancies create unique airflow pathways, allowing cooling air to bypass the pallets in distinct ways. We need to acknowledge such discrepancies when comparing with experimental data.

3.2. Analyzing a single shipment

3.2.1. Airflow in a container

3.2.1.1. AIM. We provide insight into the airflow field in a refrigerated container filled with pallets of citrus cartons (base case). Such aerodynamic information is challenging to obtain experimentally. The reasons are the limited accessibility to position the sensors, the large number of required airspeed sensors, and the challenges of measuring airflow in a stack of porous media (Geyer et al., 2018). Therefore, simulations can provide additional insights into the airflow field within the container.

3.2.1.2. Results. The airflow field is depicted in Fig. 5, with several details highlighted. Also, the pressure field in the container is depicted. The particle Reynolds number is also shown. This Reynolds number is defined based on the physical airspeed (V [m s^{-1}]) and the fruit diameter (80 mm). The inlet slot Reynolds number, based in the inlet height of the container (63.5 mm) and the inlet airflow rate (7.9 m s^{-1}) equals 34,400. This value also equals the outlet slot Reynolds number, since the airflow rate is the same. The average values and standard deviations of the superficial airspeed in the pallets and the seven-eighths cooling time (SECT) and remaining shelf life (RSL) are shown in Table 2 for all simulations, as well as the pressure drop over the computational model. Note that some components that induce a pressure loss (heat exchanger) are not included in our model, by which this pressure will be lower than the one which the evaporator fans need to deliver.

3.2.1.3. Conclusions

3.2.1.3.1. Airflow and airspeed in the container. The airflow inside the container is characterized by several main pathways toward the upper cavity and the outlet. One pathway is through porous pallets with ventilated packaging. The other pathway is via the cavity at the back of the container (door-end). The airflow bypasses via the cavity at the container's door end, even if a void plug is installed. This bypass happens as air flows through the space at the bottom of the pallets, created by the pallet base near the door end into the cavity. A void plug aims to

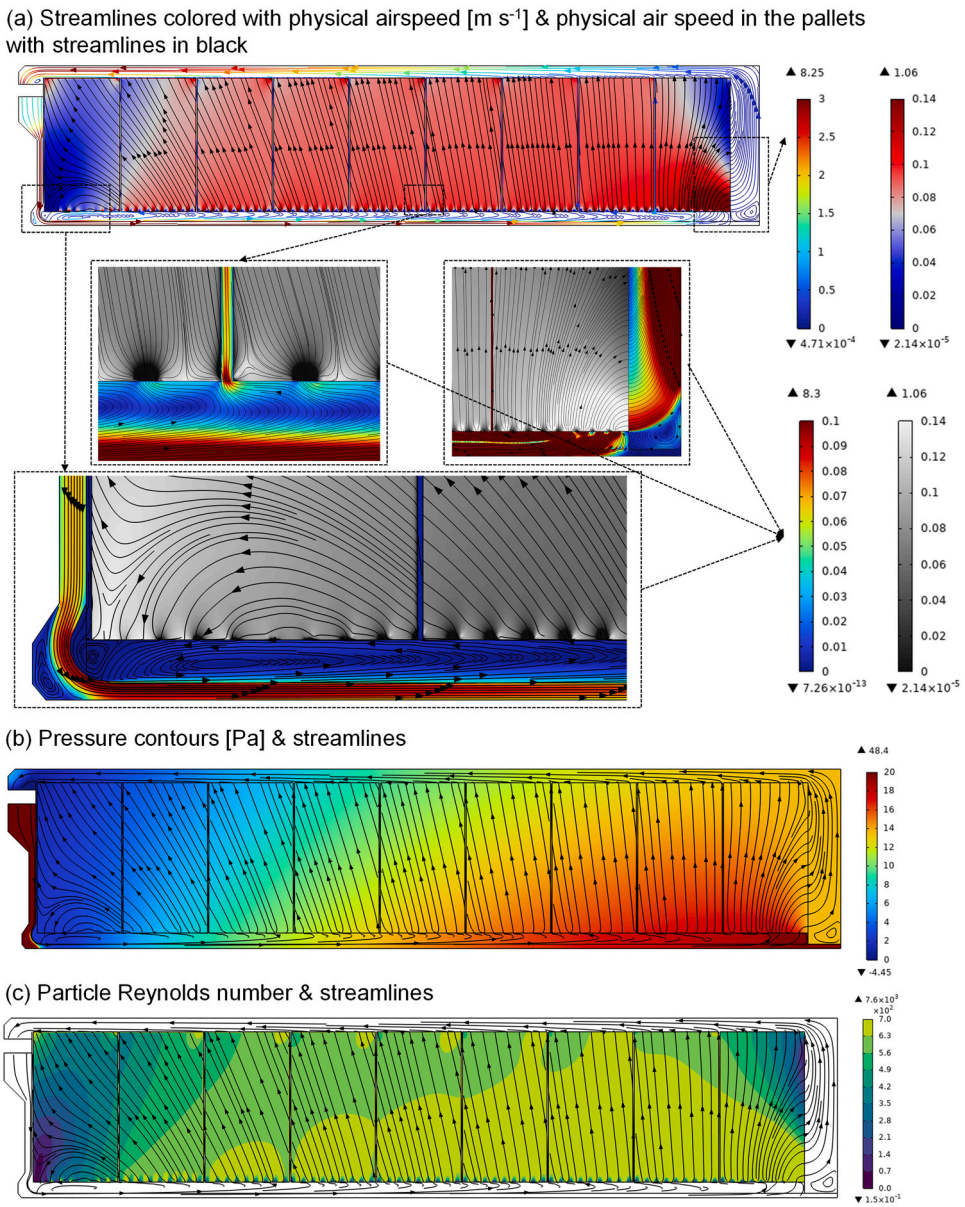

Fig. 5. (a) Airflow field in the container, focusing on different details (different scales are used in the pallets and in the air). (b) Pressure field inside the refrigerated container. (c) Particle Reynolds number. The minimal and maximal values of each color scale are indicated.

close the pallet base's open space and the open T-bar area on which a pallet is not placed at the end of the container. The plug prevents airflow from bypassing the pallets directly and traveling from the inlet to the outlet via the air cavities only. Despite this void plug, a significant portion of the air bypasses the cargo via the pallet at the door end (Fig. 5). The third pathway is airflow through the 20 mm gaps between the pallets also leads to airflow bypass.

The vertical airflow rate that goes vertically upward in the cavity between the door-end pallet and doors in a horizontal center plane at half the height of the container (y = 1.29 m, Fig. 3) is 10% of the total airflow rate at the inlet of the container (4150 m^3 h^{-1}). Due to this bypass, only 90% of the airflow passes through the pallets and gaps in this center plane. Other void plug strategies that avoid this bypass are evaluated in section 3.3.

The airspeed inside the pallets of fruit is mostly uniform, except near the door end and the refrigeration unit end of the container. The palletized fruit thereby acts as a flow straightener due to its large resistance to airflow. A low-speed zone inside the pallets appears near the top at the door end. Practitioners often report this to be the slowest cooling location inside refrigerated containers. The recirculation zone at the refrigeration unit end also induces a low-speed zone (Defraeye et al., 2022). One reason is that the high-speed air jet that enters the cargo hold via the T-bar floor remains attached to the container floor. The jet does not directly go around the corner into the first pallet. This phenomenon is due to the Coanda effect, where an air jet remains attached to a wall. The fact that the airflow is also guided in the grated T-bar floor results in the confinement of the wall jet to the bottom of the container. As a result, a recirculation zone is predicted in the air cavity where the pallet base is and inside the first pallet of fruit. The presence of this predicted recirculation zone is still a point of discussion since it seems not to be present in most full-scale experiments (Defraeye et al., 2022). A detailed discussion of this phenomenon is given in (Defraeye et al., 2022). However, the current simulation predicts the presence of this recirculation zone in a 2D container model with the k-ε turbulence model and the specific packaging and container geometry. For other simulation cases, this zone can disappear, as will be shown in sections 3.3 and 3.7.

The airflow regime is turbulent in the cargo hold, based on the particle Reynolds number. Within the fruit pallets, the average particle

Table 2
Average values and standard deviations in the different simulations for the superficial air speed in the pallets, the seven-eighths cooling time, and the remaining shelf life. The average speed in the gaps and in the void near the door end are also given as well as the pressure difference between the inlet and outlet.

Name	Specification	Superficial air speed in pallets [m s^{-1}]		Superficial air speed in gaps between pallets [m s^{-1}]	Superficial air speed in the void at door end of the container [m s^{-1}]	Seven-eighths cooling time of pallets [d]		Remaining shelf life after 5 days of transport of pallets [d]		Pressure difference inlet-outlet [Pa]	Pressure difference inlet cargo hold-outlet [Pa]
		Average	Standard deviation	Average		Average	Standard deviation	Average	Standard deviation		
Base case		0.0395	0.0118	0.344	0.101	1.01	0.48	13.82	0.11	47.7	15.1
Airflow rate	50%	0.0192	0.0054	0.183	0.038	1.86	0.94	13.64	0.21	12.3	3.9
	25%	0.0095	0.0025	0.098	0.014	4.96	5.03	13.31	0.36	3.2	1.0
	150%	0.0609	0.0182	0.503	0.172	0.73	0.33	13.89	0.07	105.8	33.7
Gaps	0 mm	0.0441	0.0123	0.000	0.087	0.95	0.43	13.83	0.10	48.1	15.6
	10 mm	0.0427	0.0121	0.210	0.094	0.96	0.45	13.83	0.10	48.1	15.5
	20 mm	0.0395	0.0118	0.344	0.101	1.01	0.48	13.82	0.11	47.7	15.1
	40 mm	0.0330	0.0108	0.434	0.127	1.18	0.56	13.79	0.13	46.6	14.0
	60 mm	0.0283	0.0097	0.440	0.255	1.40	0.64	13.75	0.14	45.8	13.3
Void plug strategies	Void plug bottom (base case)	0.0395	0.0118	0.344	0.101	1.01	0.48	13.82	0.11	47.7	15.1
	No void plug	0.0256	0.0087	0.210	0.549	1.59	0.77	13.71	0.18	46.3	13.8
	Void plug bottom & top	0.0406	0.0114	0.354	0.067	0.99	0.46	13.83	0.11	47.8	15.2
	Full void plug	0.0425	0.0109	0.370	0.000	0.96	0.44	13.83	0.10	48.0	15.4
	Full void plug - top open	0.0425	0.0109	0.370	0.000	0.96	0.45	13.83	0.10	48.0	15.4
	Full void plug - top open - bleed flow	0.0377	0.0093	0.321	0.394	1.05	0.49	13.81	0.11	47.4	14.9
Loading container with partially-precooled cargo		0.0395	0.0118	0.344	0.101	0.86	0.45	13.87	0.09	47.7	15.1
Height T-bar floor adjusted	42.3 mm	0.0463	0.0139	0.413	0.117	1.37	0.67	13.78	0.14	84.2	32.5
	50.8 mm	0.0432	0.0141	0.370	0.115	1.28	0.75	13.78	0.16	68.2	25.2
	63.5 mm (base case)	0.0395	0.0118	0.344	0.101	1.01	0.48	13.82	0.11	47.7	15.1
	79 mm	0.0389	0.0097	0.370	0.090	0.97	0.40	13.83	0.10	40.8	12.1
	95 mm	0.0392	0.0094	0.390	0.072	0.96	0.41	13.83	0.10	38.5	12.4
	127 mm	0.0403	0.0171	0.433	0.037	1.08	0.64	13.81	0.14	44.0	19.2
	127 (pallet height reduced)	0.0389	0.0103	0.386	0.071	0.96	0.43	13.83	0.10	31.1	6.3

Reynolds number is 599. At particle Reynolds numbers above 100–300, flow around a sphere does not remain laminar (Defraeye et al., 2013; Jones and Clarke, 2008). As such, the flow inside the pallets cannot be considered laminar.

3.2.1.3.2. Pressure loss. The pressure loss between the inlet and the outlet of the computational domain (inlet to outlet) is 48 Pa and that over the cargo hold is 15 Pa, so from the inlet at the T-bar floor until the outlet. The pressure loss over the cargo hold seems small, in contrast to the intuitively large airflow resistance that the airflow encounters when flowing through the pallets of fruit. However, the physical air speed in the cargo hold is typically very low (Fig. 5). This speed is more than a factor of 100 lower than at the inlet slot of the cargo hold at the T-bar (7.9 m s^{-1}) and the inlet duct in the refrigeration unit. The pressure drop over the pallets at these speeds is therefore limited. The packaging used was also well-ventilated and had a rather low-pressure resistance. Also, note that perfect stacking was assumed in the simulations, and packaging was not stacked staggered on the pallet. Higher pressure drops can occur over the packaging for other package types and container loading strategies.

The T-bar floor and the wooden pallet base have a limited effect on the pressure losses. Omitting them only reduced the pressure loss over the cargo hold by about 10% (results not reported). Their impact on the airflow field and fruit cooling was negligible.

A large part of the momentum loss occurs in the refrigeration unit due to the high airspeeds and obstructions. The airspeed in the refrigeration unit is roughly a factor of 100 times larger than in the porous cargo. Since the pressure loss increases quadratically with the airspeed, the pressure loss over a certain obstacle in the refrigeration unit will be much higher than over the same obstacle in the cargo hold. Practically, this implies that the pressure increase that the fans deliver is mainly required to force air through the refrigeration unit into the cargo hold. Loading the container with different types of packaging will, thus, not drastically change the operation point of the fans and the impact on the airflow rate. However, the container evaporator fans typically deliver an even higher pressure rise (~ 40–200 Pa, (Defraeye et al., 2024)), compared to the pressure losses found in our simulations. The reason is that some components that induce a pressure loss in the return air section, such as the heat exchanger, are not included in our model.

3.2.1.4. Cooling and food quality uniformity within a shipment

3.2.1.4.1. Aim. The food quality evolution and the resulting remaining shelf life are reported and provide insight into the cargo's cooling process in a refrigerated container. We quantified the uniformity of these parameters throughout the cargo. We simulated an idealized case of ambient loading where the set point temperature remains constant (base case). Currently, this information is unavailable from experiments on that spatial resolution, so simulations can provide additional insights into the food cooling within the container.

3.2.1.5. Results. The temperature in the air and the fruit are depicted at several points in time in Fig. 6, and the difference between fruit and air temperature in the pallets is shown in Fig. 7. The distribution of the temperature-driven quality index of the fruit in the pallets after 5, 10, 15, 20, and 24 days is shown in Fig. 8. The resulting seven-eighths cooling time is depicted in Fig. 9. The remaining shelf life after the full transport period of 24 days is shown in Fig. 9, together with the streamlines. A streamline is the path that would be followed by a massless particle when it moves with the flow. Note that SECT and RSL are calculated based on the fruit pulp temperature. The volume-averaged fruit temperature is assumed to equal the core pulp temperature. The fruit pulp temperature is calculated to be uniform in our two-phase porous medium simulation study, which is justified due to the low Biot numbers. The Biot number distribution is shown in Fig. 9. The Biot

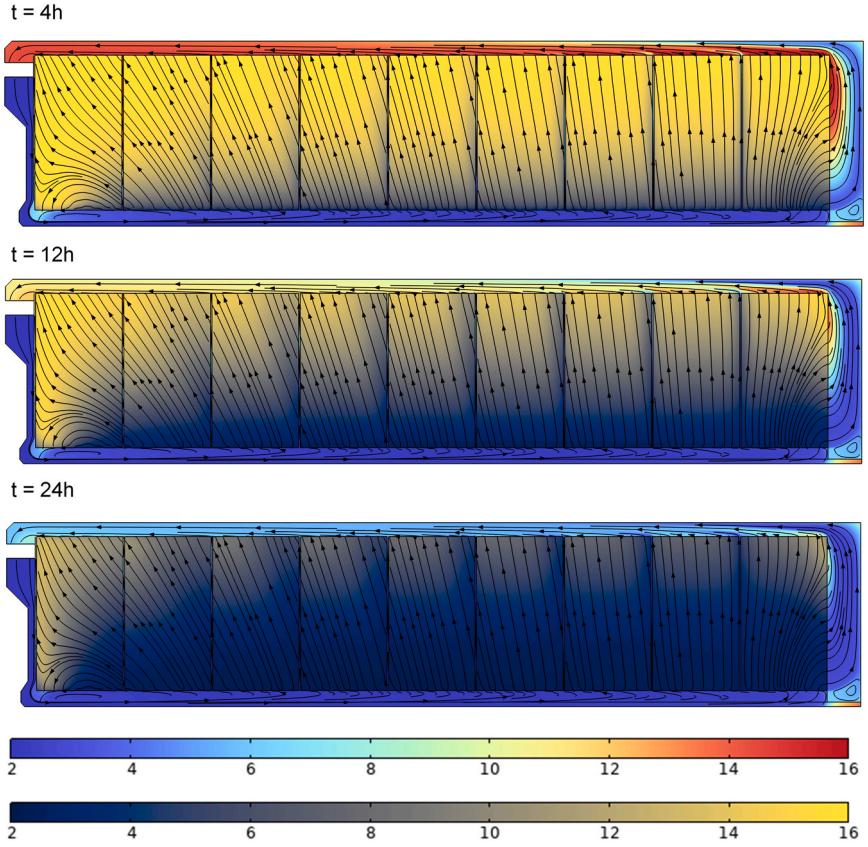

Fig. 6. Air temperature [°C] in the cavities in the air domain (rainbow color scale), streamlines, and fruit temperature (blue-to-yellow color scale) in the pallets after 4, 12, and 24 h.

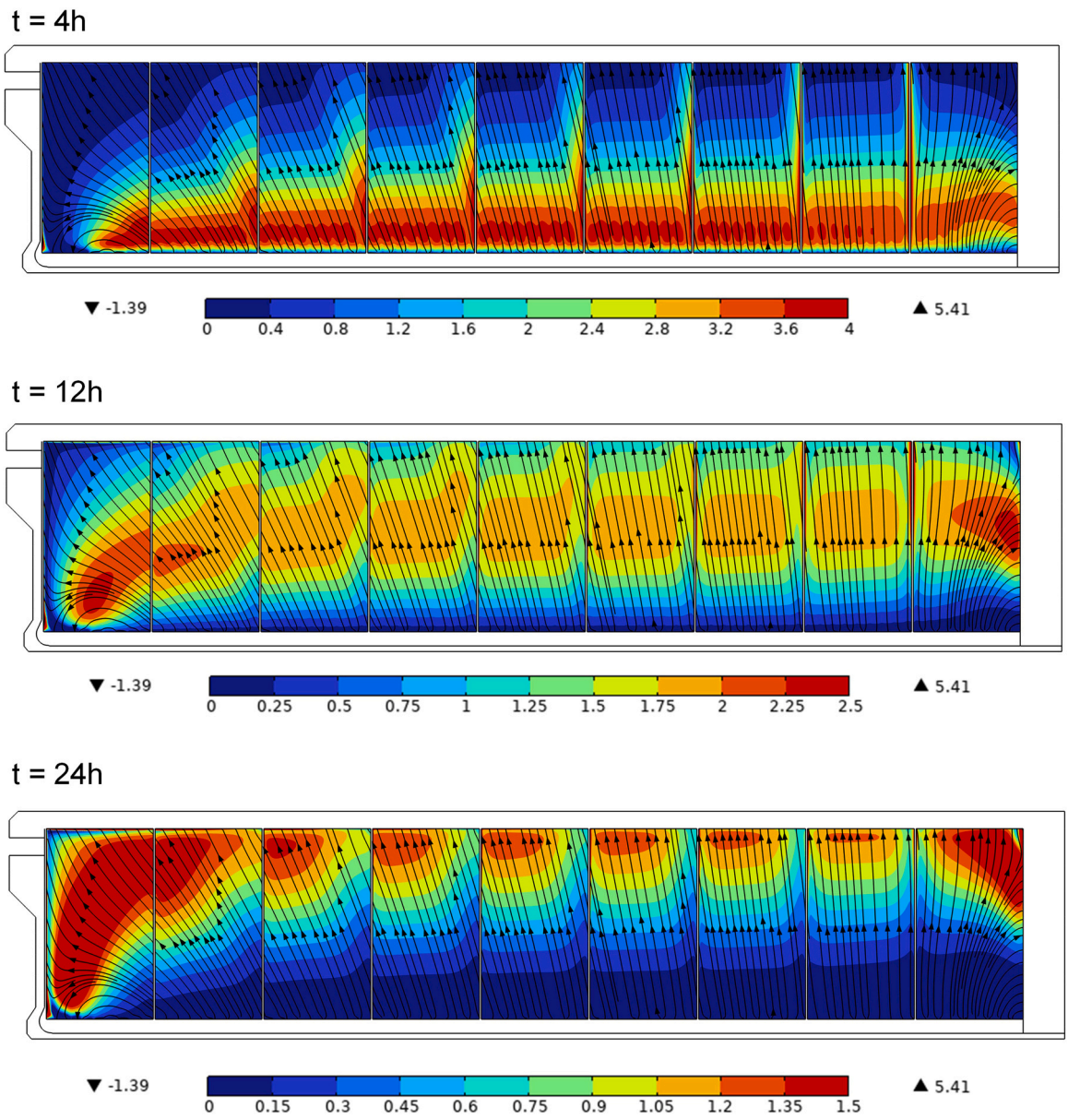

Fig. 7. Difference between the fruit and air temperature [°C] and streamlines in the pallets after 4, 12, and 24 h.

number is defined as the ratio of the convective heat transfer coefficient h_c [W m^{-2} K^{-1}] and the characteristic length L_H [m] to the thermal conductivity of the solid (fruit) λ_s [W m^{-1} K^{-1}]. The characteristic length is estimated as the ratio between the product's volume V [m^3] and the surface area from which heat is exchanged with the environment A_s [m^2]. This length equals $r_p/3$, where r_p is the fruit radius [m]. The Biot number depends on h_c, and thus on the local airspeed. The remaining shelf life was calculated assuming the fruit was stored at 23 °C after the shipment arrived. We also quantitatively evaluated the distribution of the SECT and RSL of multiple fruits by placing virtual fruit probes in 58,860 locations in the cargo. This distribution of the SECT, quality index, and RSL is shown in Fig. 10.

3.2.1.6. Conclusions. The slowest locations for cooling and the lowest remaining food quality are the fruit at the top of the pallets as the bottom fruit cools the fastest. Two pallet rows exhibit slower cooling, leading to a reduction in the predicted fruit quality. These pallets are positioned near the door end and also closest to the refrigeration unit. The driver for these slowest cooling locations is the low airspeeds in these regions (Fig. 5). Note that the simulated low cooling rates of the pallet near the refrigeration unit end are often not found in experiments (section 3.2.1). A detailed evaluation on this phenomenon is given in (Defraeye et al., 2022). However, for our specific 2D computational setup, turbulence modeling, and specific packaging and loading strategy, we predict the presence of this recirculation zone. In addition to these locations with the slowest cooling, a high-air-temperature zone is found between the floor and the void plug at the bottom of the container near the door end. The reason is that the heat from the outside is trapped between the floor and the void plug and is only slowly removed (Fig. 6). Also note that heat still enters the cargo hold at the end of the cooling process via the container walls, despite their insulation. As such, the air in the T-bar floor heats up slightly after entering the cargo hold.

Upon arrival, these locations, pallets, and boxes or 'hot spots' should be prioritized for fruit quality inspection. These pallets are also the preferred locations to place the sensors for monitoring the cargo. They are considered to be conservative locations to probe if problems with the shipment can be expected. Both air temperature and fruit pulp temperature sensors can be used to pick up these anomalies. We discussed the slowest cooling locations. On the other hand, the locations where

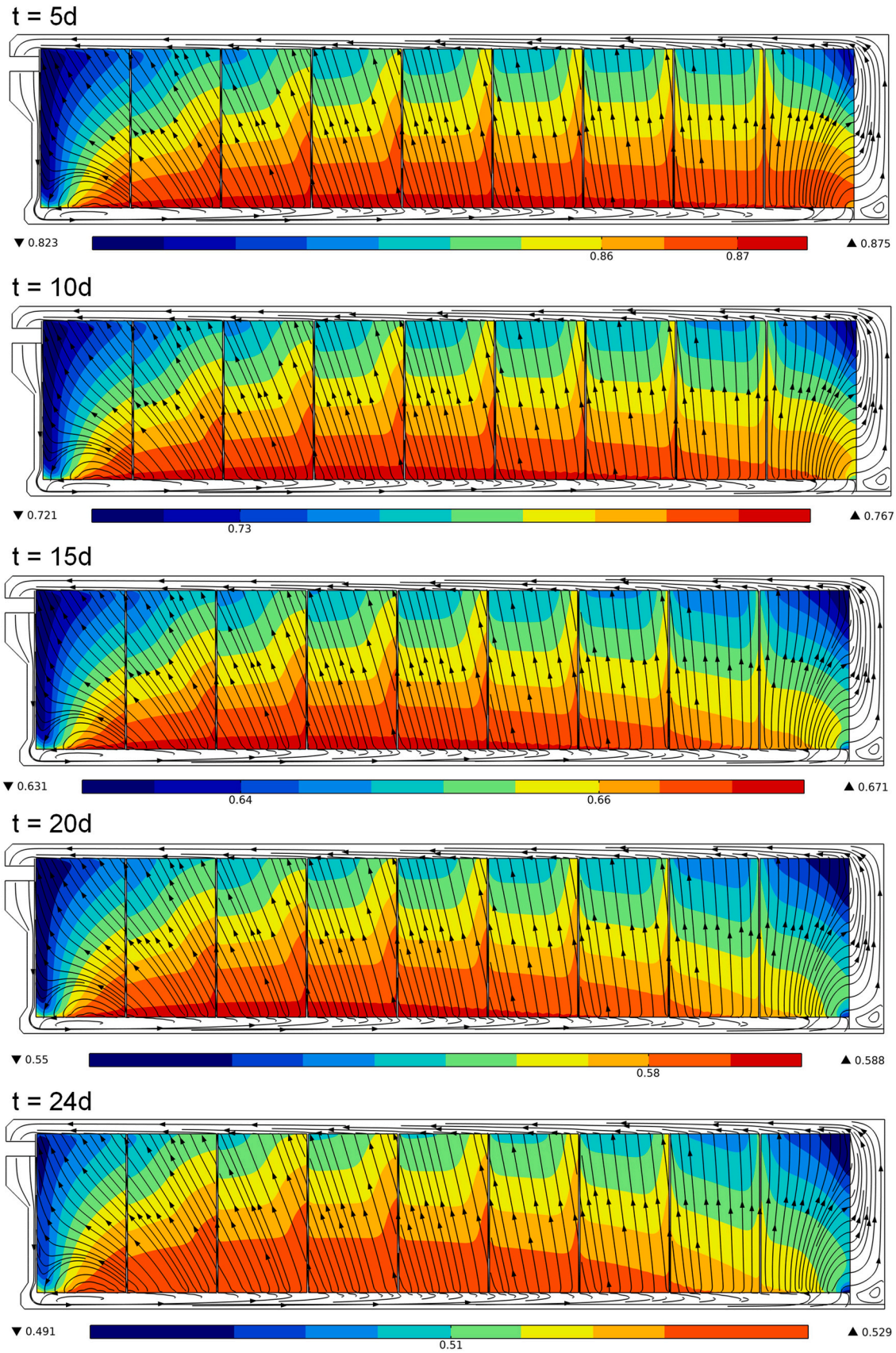

Fig. 8. Distribution of the quality index (ranging between 0 and 1) of the fruit and streamlines in the pallets after 5, 10, 15, 20, and 24 days. The minimal and maximal values are indicated. Note that the variations within a specific plot are rather small.

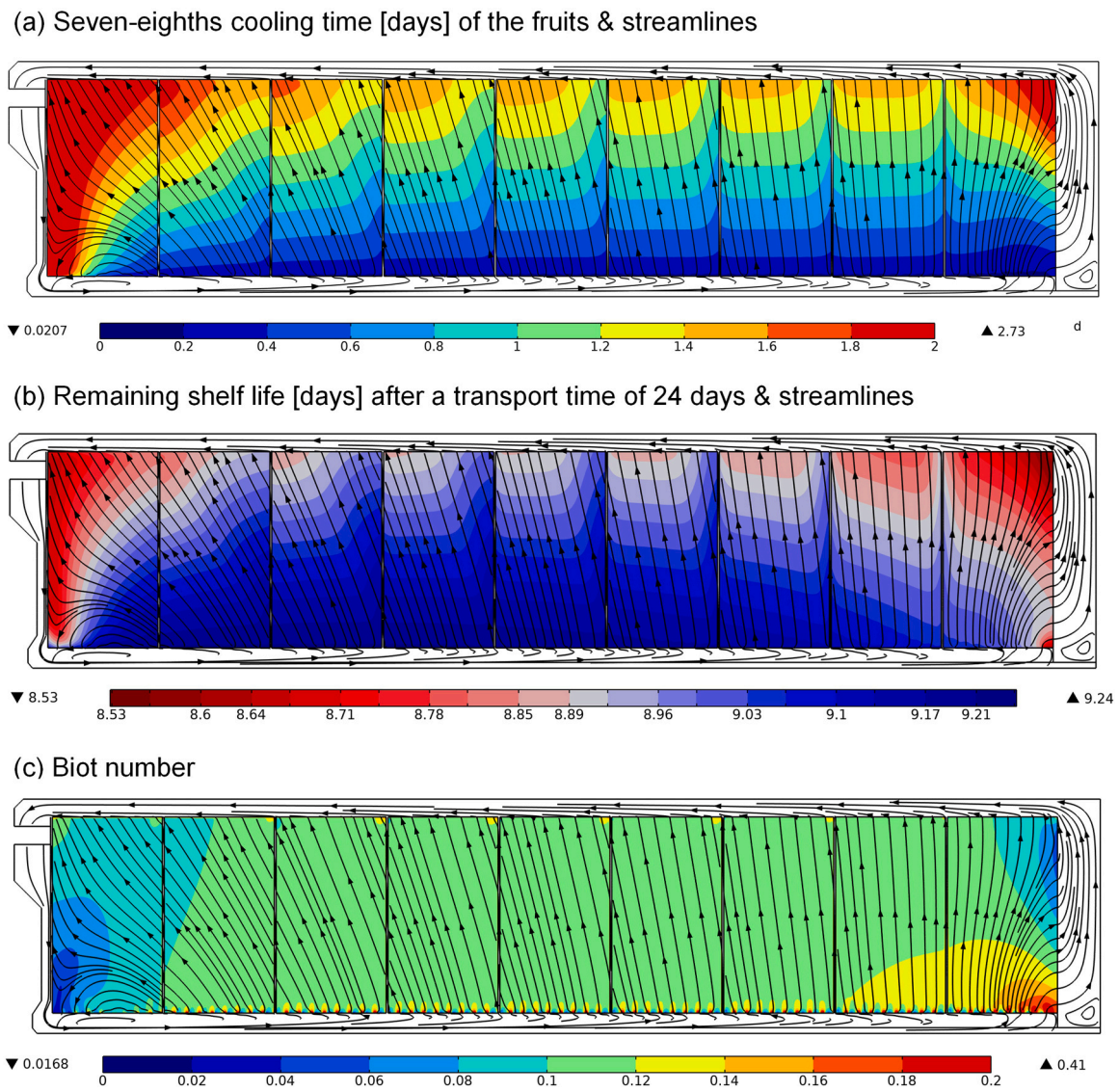

Fig. 9. (a) Seven-eighths cooling time distribution [days] in the fruit pallets and streamlines. (b) Remaining shelf life [days] after a transport time of 24 days and streamlines. (c) Biot number distribution inside the cargo, based on physical airspeed and streamlines.

chilling injury will most likely be found are at the bottom of the pallets, as here, the coldest temperatures are found. Therefore, the locations for chilling injury incidence and likely also mass loss will be at a different location in the container than that for high-temperature-related fruit quality losses such as decay.

The non-uniformity in SECT and RSL throughout the cargo was substantial. The difference in SECT within the cargo between the minimal and maximal values was over 2 days. The difference in remaining shelf life after the transport period of 24 days was about 0.7 days. As such, not all fruit cool at the same rate resulting in different qualities. When consumers would choose fruit from a carton at the bottom of a pallet, compared to the carton at the top of the pallet at the door end, fruit could last longer at home, given that no chilling injury occurred. The RSL, however, seems to exhibit smaller differences throughout the cargo than the SECT. For orange fruit, fruit quality loss has a much longer time scale than a cooling process (Defraeye et al., 2024). This implies that quality loss processes occur slower than fruit cooling (Defraeye et al., 2019). As such, spatial differences in cooling within the cargo may not necessarily reflect a pronounced fruit quality reduction. Using virtual probes, the distribution of the SECT and RSL was also mapped and statistically analyzed in the histogram (Fig. 10). The SECT distribution is rather symmetrical but not normally distributed. A long tail appears due to the two pallets that cool slower. The RSL distribution throughout the cargo is also skewed. There is a cutoff for high-quality fruit as, given at a certain delivery air temperature, the fruit that cool down the fastest cannot exceed a certain quality. When looking at the transient cooling process (Fig. 7), the fruit is warmer than the air entering the pallets at the start of the cooling process. However, the fruit at the bottom is cooled down rather rapidly. As such, the highest differences in air and fruit pulp temperature are found in the top cartons after 24 h.

Interestingly, the distribution of the remaining shelf-life depends on when the fruit were evaluated (Fig. 10c), even after all fruit are cooled down during the first days. This originates from the fact the quality index of the fruit varies within the cargo after the cargo has been cooled down (Fig. 8). As a result, fruit evolve to a different quality when transported afterward at the same constant temperature. The quality loss after a certain number of days will depend on the initial quality index after cooling since the quality decay is non-linear. Fruit with a higher quality index after cooling will lose in a period of 5 days, for example, more than fruit at a lower quality. So even if the cargo is cooled down, the quality index and RSL will develop differently throughout the

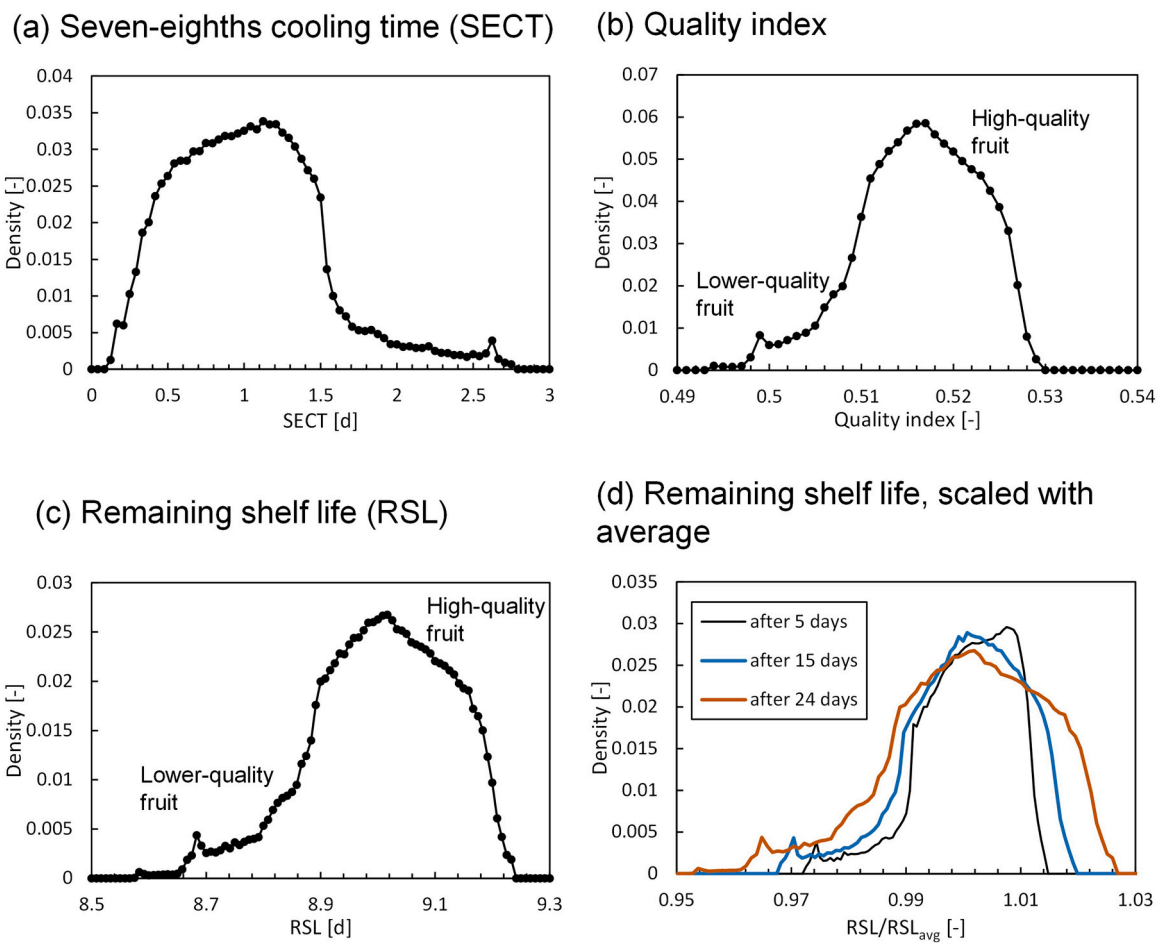

Fig. 10. Histogram of seven-eighths cooling time (a), quality index (b) and remaining shelf life after 24 days (c) for 58,860 virtual fruit pulp probes inside the cargo. The RSL, scaled with the average RSL over the cargo, is shown (d) for different moments in time.

cargo (Fig. 8, Fig. 10c). In summary, the time after shipping when the RSL distribution is evaluated will determine how the shape of the RSL histogram looks (Fig. 10c). We cannot offset the histogram with a constant value. The changes between the histograms with time are, however, rather small.

The Biot number is about 0.10 within the cargo at the maximum airflow rate the container fans can deliver. This low value implies that the thermal gradients inside the fruits are limited. Using a two-phase approach for modeling the porous medium without including internal thermal gradients inside each fruit (Defraeye et al., 2024) thus approximates the physics of the cooling process appropriately.

3.3. *Impact of airflow rate on cooling and food quality uniformity within a shipment*

3.3.1. *Aim*

We answer to which extent the cargo cools faster and more uniformly in a refrigerated container when the fans are operated at a high-airflow regime compared to when operated at a low-airflow regime. The low-speed regime is typically 50% of the airflow rate at normal speed (4150 m^3 h^{-1}). High airspeeds typically improve cooling rates and uniformity between the different fruit throughout ventilated packaging (Defraeye et al., 2015a; Wu et al., 2018). However, low airflow rates are preferred by shipping lines during transport to reduce power consumption so energy use by the evaporator fans and also to limit moisture loss. Automatic switching to low airflow rates is implemented in control protocols of refrigerated containers. However, this energy-saving mode can negatively affect the quality of the cargo when it is not completely cool. The trade-off between saving energy and optimally maintaining fruit quality is not routinely analyzed as it is challenging to quantify the resulting quality loss of the cargo. Secondly, we aimed to explore the impact of the speed on the flow field and cooling in a broader sense. Therefore, we also evaluated an airspeed that is outside the container's current range, namely 25% and 150% of the actual airflow rate.

3.3.2. *Results*

The scaled seven-eighths cooling time, airspeed distribution, and RSL after 5 days are depicted in Fig. 11 for all container air speeds, together with the streamlines. The SECT is scaled here with the average SECT of the cargo. We also quantitatively evaluate the distribution of the SECT and RSL of multiple fruits by placing virtual fruit probes in 58,860 locations in the cargo and shown in Fig. 12. The average values and standard deviations of the superficial airspeed in the pallets as well as the SECT and RSL, are shown in Table 2.

3.3.3. *Conclusions*

The cargo cools down about 0.8 days and 3.9 days slower (in terms of SECT) at 50% and 25%, respectively, than at the high airflow rate (100%) in the container. However, the impact on the fruit quality is more limited since citrus fruit is very robust compared to more perishable fruit types. The fruit quality was not excessively compromised at lower airspeeds, and we lost about 0.18 d and 0.33 d more of RSL on average, at 50% and 25%. The variability in food quality within the cargo are limited, but we see a larger variability at low airflow rates. Following previous findings, the cooling uniformity increases at higher airflow rates, as the standard deviation in the SECT in the cargo was 47%

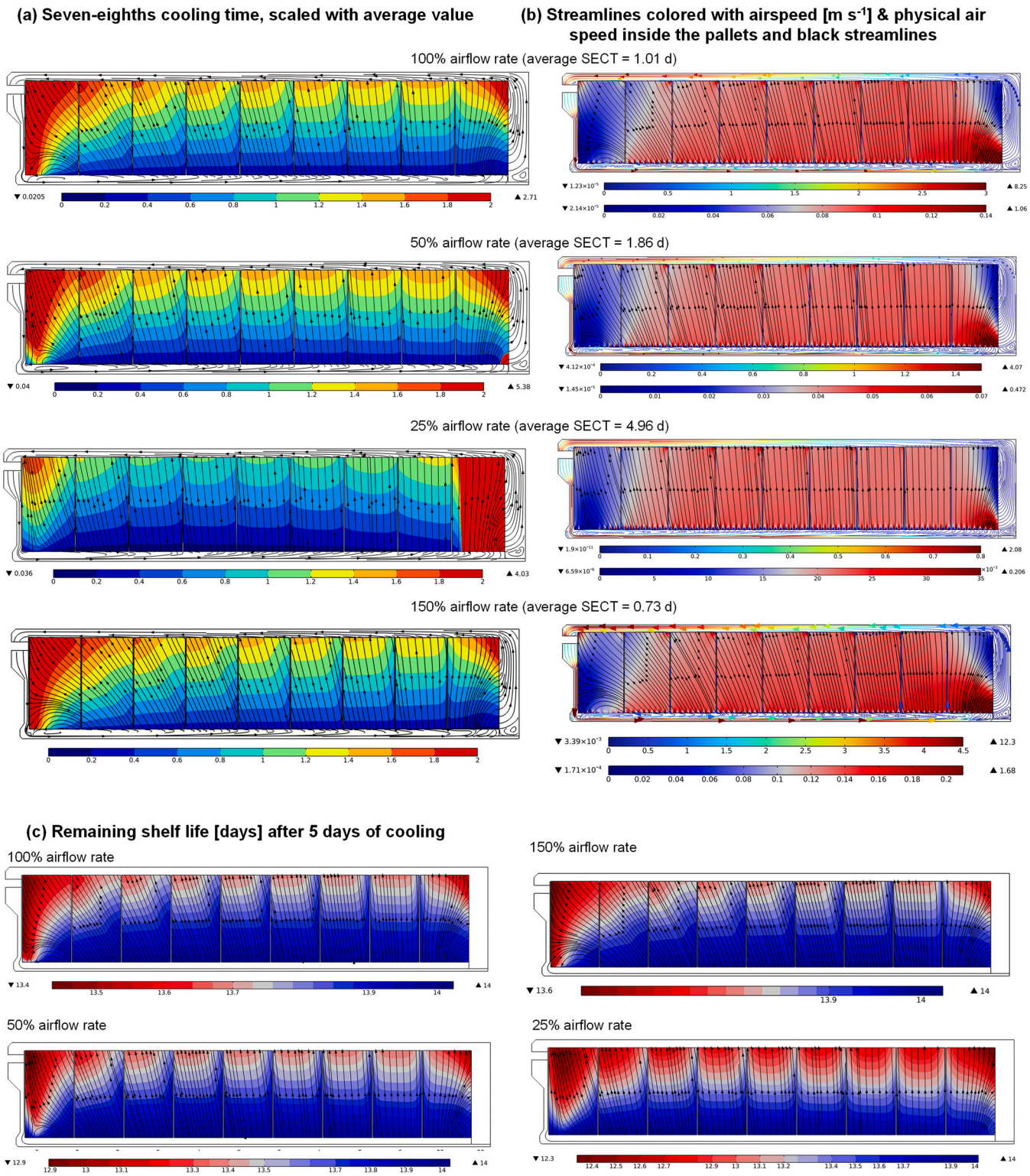

Fig. 11. (a) Seven-eighths cooling time distribution in the fruit pallets, scaled with the average value over all pallets and streamlines. (b) Physical air speed inside pallets (waveclassic color scale) and streamlines in air, colored with airspeed (rainbow color scale). (c) Remaining shelf life after 5 days of cooling (scale differs for each graph).

vs. 102% of the average value for high (100%) and low (25%) airflow rates, respectively. At higher airflow rates (150%), the cooling uniformity becomes even better. Note that a phytosanitary protocol for citrus fruit can only start when the cargo is cooled to a specific temperature. Therefore, the cargo needs to be cooled as fast as possible.

At lower airspeeds, the recirculation zone near the bottom at the refrigeration unit end almost completely disappears, which leads to a better quality retention at the bottom of the pallet, relative to the rest of the cargo. The relative airflow that bypasses the pallets is about the same at each airspeed (results not shown), so this is not affecting the differences between the different speeds so much.

Note that the SECT is not reached at the door end of the container at

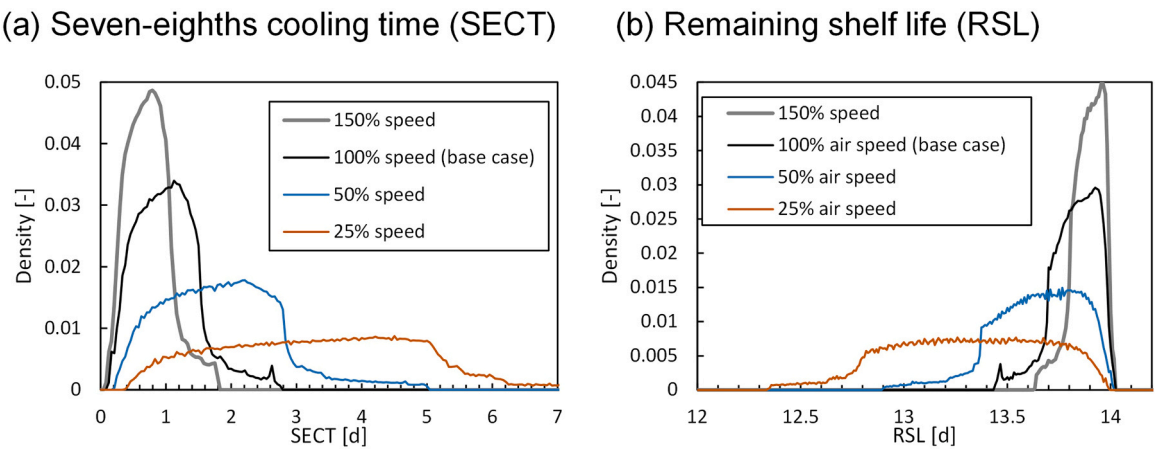

Fig. 12. Histogram of SECT (a) and RSL after 5 days (b) for 58,860 virtual fruit pulp probes inside the cargo for different airflow rates at the inlet.

low air speeds. The reason is that, apart from the low airspeeds, the air in the T-bar floor heats up slightly due to the heat from outside. As a result, slightly warmer air enters the pallets at the door end. Although the pallets are cooled down rather fast, the SECT is reached much later since it is defined based on the inlet temperature.

In conclusion, cooling at higher airflow rates better preserves quality and uniformity but will come at a higher energy cost due to running the evaporator fans. Therefore, it is advised that, during warm loading or 'hot stuffing' of the container, high airflow rates are used for the first three days.

3.4. Impact of gaps between pallets on cooling and food quality uniformity within a shipment

3.4.1. Aim

We aim to quantify to which extent gaps between the pallets affect the airflow pattern in the container, the resulting fruit cooling, and fruit quality during ambient loading or 'hot stuffing' of the cargo.

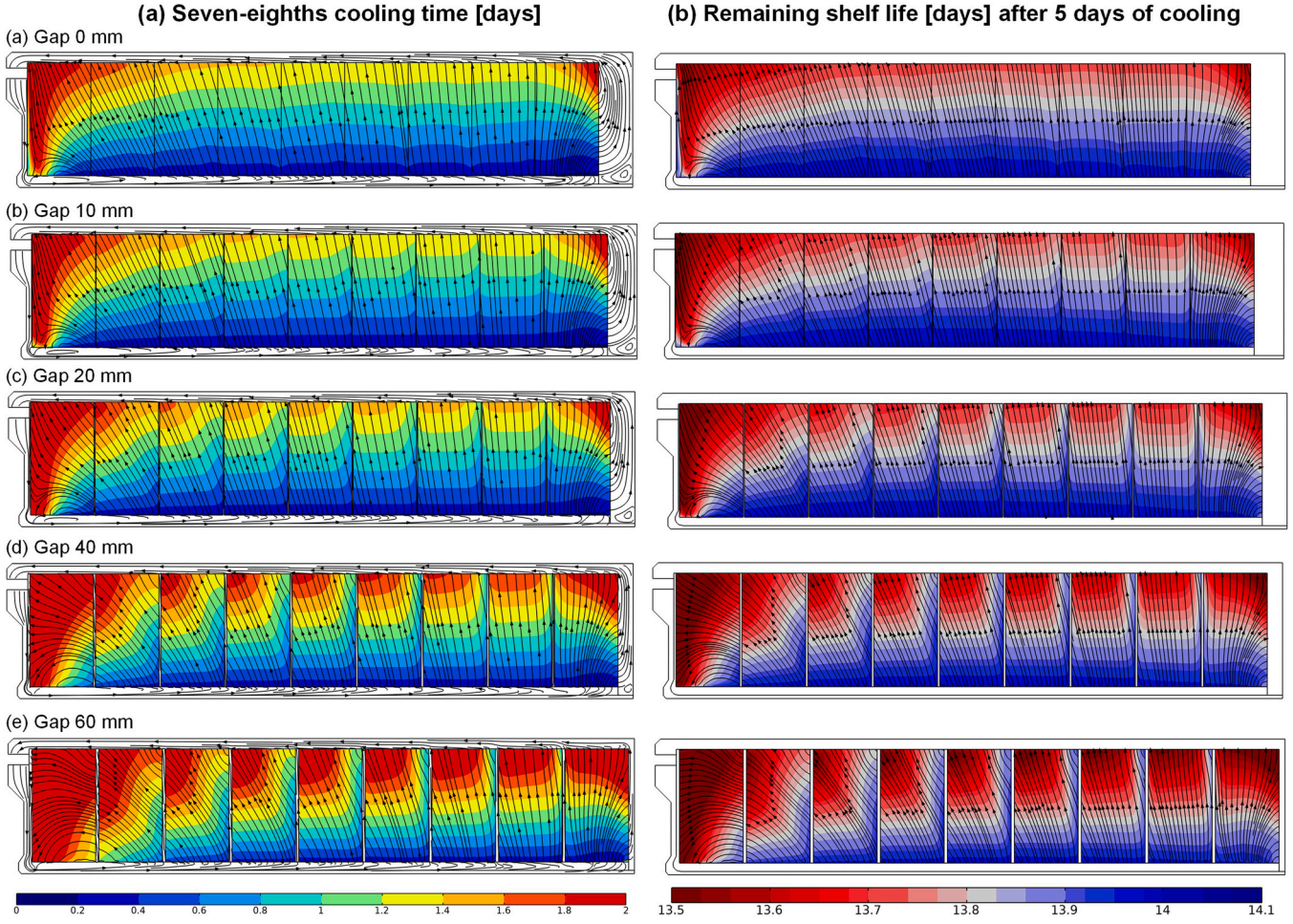

Fig. 13. Seven-eighths cooling time distribution (a) and RSL after 5 days of cooling (b) in the fruit pallets and streamlines for different gap sizes between the pallets.

3.4.2. Results

Fig. 13 shows the SECT and RSL results of a cargo without gaps between the pallets and with different gap sizes, namely 10 mm, 20 mm (base case), 40 mm, and 60 mm. We also quantitatively evaluate the distribution of the SECT and RSL of multiple fruits by placing virtual fruit probes in 58,860 locations in the cargo. This distribution of the SECT and RSL is shown in Fig. 14. The average air speeds in the pallets, the gaps, and the air void at the door end of the container are shown in Fig. 15. The average values and standard deviations of the superficial airspeed in the pallets as well as the SECT and RSL, are shown in Table 2.

3.4.3. Conclusions

The fastest cooling and best quality preservation are achieved when no gaps exist. The average SECT without gaps and with gaps of 60 mm are 1.01 + /- 0.48 and 1.40 + /- 0.64 days, respectively. The average RSL after 5 transport days are 13.82 and 13.75 days, respectively. Air gaps between the pallets seem to greatly impact fruit cooling but less fruit quality. Again, the reason is the differences in time scales between cooling and quality loss. Gaps reduce the cooling rate due to a significant amount of cold air bypassing the pallets' fruit via these gaps. The airspeed in the pallets steadily decreases with gap size (Fig. 15). As such, the pallets' superficial and physical air speeds are reduced, so the cargo cools slower. The average superficial airspeed in the pallet is 0.044 m s^{-1} when no gaps are present, compared to 0.028 m s^{-1} with 60 mm gaps. This is a reduction of 36%. The airspeed in the gaps between the pallets increases with gap size until 40 mm, where an asymptote seems to be reached (Fig. 15). The airspeed in the void at the back becomes larger here. Note that the airspeed in the gaps and the void is an order of magnitude larger than in the pallets.

In contrast to the negative effect of gaps on the cooling, due to airflow bypass, the gaps locally increase the cooling rate of the pallets at the edges of the pallets. This effect seems very local and does not offset the bypass effect. We work with a 2D model. In reality, the gaps are also present on the pallets' sides. Therefore, the current results are indicative, but a 3D simulation would be more representative to assess this local cooling effect.

In summary, the positive effect of local cooling and ventilation at the pallet edges does not outweigh the additional cold air bypass. This bypass air is not used to cool the cargo. It is advised to avoid airflow bypass as much as possible to have the highest airflow rate through the pallets by reducing the gaps between the pallets. The additional cooling effect that gaps or chimneys provide is very local and seems detrimental to the cooling of the rest of the cargo.

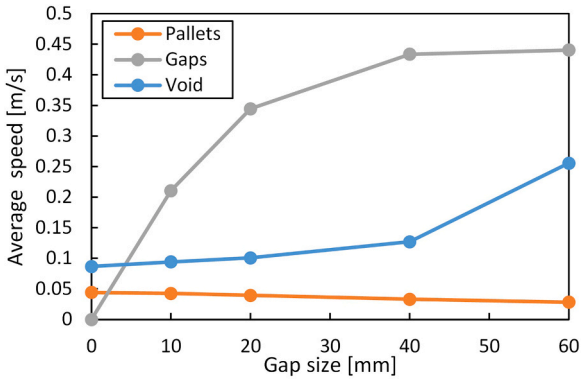

Fig. 15. Average superficial air speed through the pallets, the gaps between the pallets and the void at the door end of the container for different gap sizes.

3.5. Impact of void plug types on cooling and food quality uniformity within a shipment

3.5.1. Aim

We quantify the efficacy of void plugs to improve the cargo's cooling speed and uniformity in a refrigerated container and the resulting fruit quality. Five different variants are evaluated in addition to the normal void plug scenario and are depicted in Fig. 16: no void plug, a normal void plug on the bottom, a normal void plug combined with one at the top, a void plug covering the full pallet side and pallet as well as the top of the cavity, a void plug covering the full pallet side but with the top left open, and a void plug covering the full pallet side so with the top left open, but with a small hole at the bottom to enable some bleed flow passing through the void at the door end.

3.5.2. Results

The seven-eighths cooling time of the cargo is shown in Fig. 16 for all void plug types, together with the streamlines. Table 2 shows the average speed inside the fruit pallets, the average SECT, the average RSL, and all standard deviations from these values. The pressure difference between the inlet and outlet is also shown.

3.5.3. Conclusions

Using a void plug on the pallet base (Fig. 16b) significantly improves the cooling rate and uniformity compared to no void plug (Fig. 16a). The impact on fruit quality is more limited. The void plug eliminates the air's ability to circumvent the cargo via the T-bar floor and the pallet base zone. For the gaps between the pallets, we already quantified the detrimental effect of airflow bypass on cooling. The average superficial

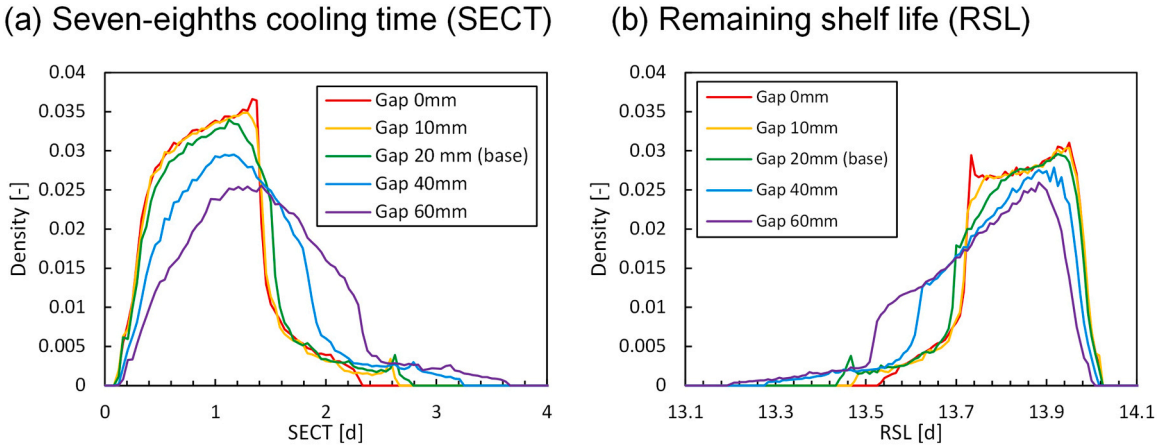

Fig. 14. Distribution of SECT (a) and RSL after 5 days (b) for 58,860 virtual fruit pulp probes inside the cargo for different gap sizes between the pallets.

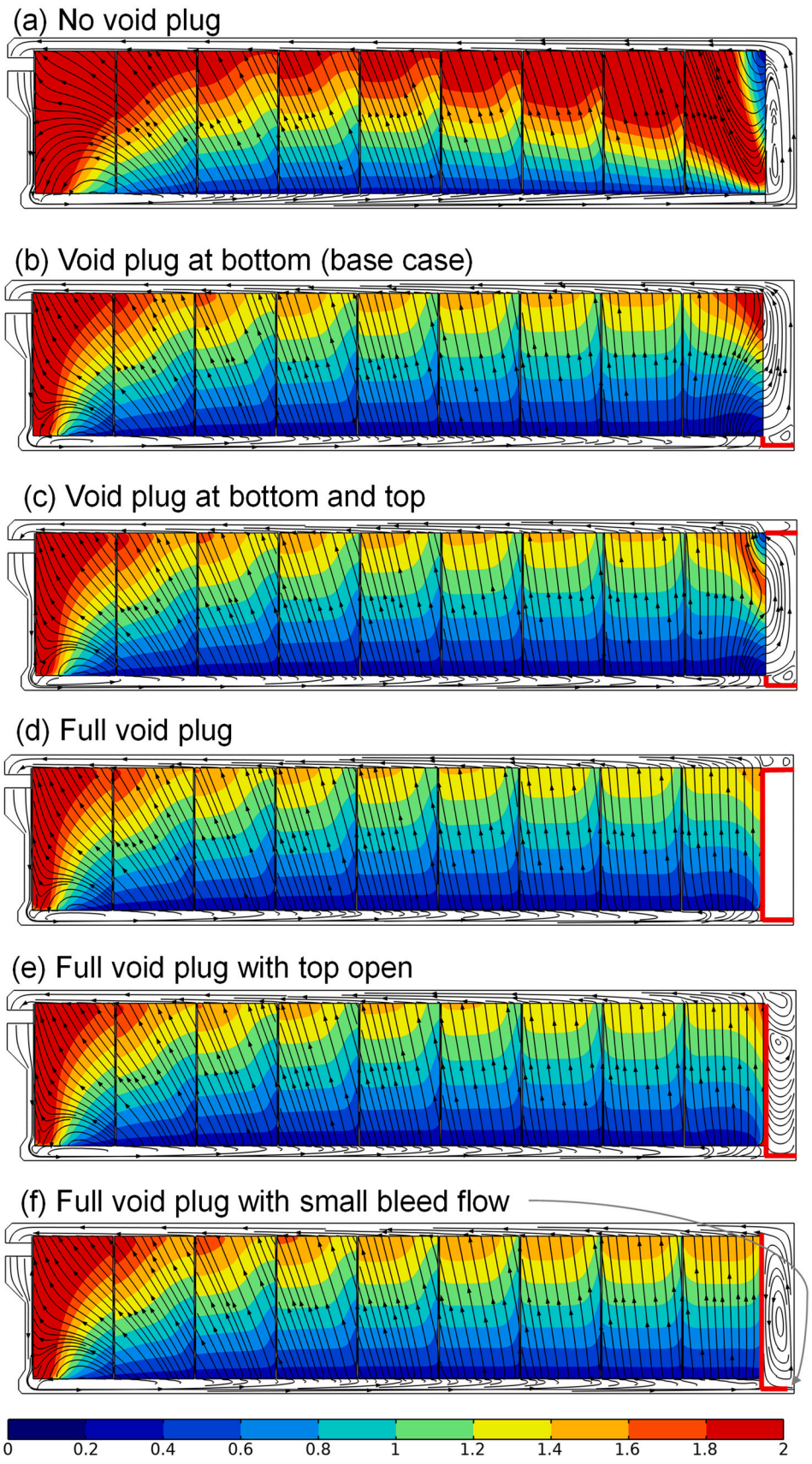

Fig. 16. Seven-eighths cooling time distribution [days] in the fruit pallets for several void plug strategies and streamlines. Void plug locations are indicated with red lines.

air speed in the pallets, which is a proxy for the airflow bypass, significantly increases when using a void plug, namely from 0.0395 m s^{-1} compared to 0.026 m s^{-1}, so by about 50% (Table 2). Adding a void plug at the top (Fig. 16c) does not induce a lot of improvement. We can also block the side of the pallet from airflow penetrating the cavity at the door end. When the cavity is fully blocked (Fig. 16d), a small gain in cooling rate is achieved. When we allow some access of the cooling air to the cavity at the back, a slight improvement is seen (Fig. 16e). A small perforation can be made in the void plug (Fig. 16f) to cool down the cavity faster. The result is a significant amount of bypass, leading to non-uniform cargo cooling. With any void plug strategy, the pressure the fans need to deliver is slightly higher than without a void plug.

The main conclusion is that using a void plug at the pallet base benefits fruit cooling rate, uniformity, and hence fruit quality retention, despite slightly increasing the pressure resistance in the cargo hold (Table 2). All additional efforts to avoid airflow bypass have a more limited effect. We also conclude that the presence of a void plug changes the slowest cooling location inside the cargo away from the last pallet at the door end. It could be beneficial to use a slightly vertically-extended void plug. This can avoid air bypassing via the pallet into the void at the door end and will improve cooling, but it does not require fully covering the side of the pallet.

3.6. Impact of loading the container with partially-precooled pallets on cooling and food quality uniformity within a shipment

3.6.1. Aim

We explore if mitigating the slowest cooled locations in the cargo and the associated accelerated quality loss is possible. To do so, the idea is to replace the critical pallets at these locations with precooled pallets. That way, we can proactively avoid these critical locations and the suboptimal fruit cooling and quality preservation.

3.6.2. Results

The RSL and air temperature after 6 h of cooling are shown in Fig. 17 for the base case and a simulation where the pallet at the door end and at the refrigeration unit end has been fully precooled to the delivery air temperature before loading it into the container. We also quantitatively evaluate the distribution of the SECT and RSL of multiple fruits by placing virtual fruit probes in 58,860 locations in the cargo. This distribution of the SECT and RSL is shown in Fig. 18. The average values and standard deviations of the superficial airspeed in the pallets as well as the SECT and RSL, are shown in Table 2.

3.6.3. Conclusions

The slowest cooling locations disappear upon precooling the pallets corresponding to these locations inside the cargo. The SECT distribution becomes more uniform, and the long tail with a long cooling time disappears. Also, the tail in the RSL distribution disappears. In summary, precooling a part of the cargo and placing these cooled pallets at the key locations renders the cooling and the quality of the fruit in the cargo more uniform. This strategy can help mitigate quality problems in the pallets near the door end or other critical locations and is essentially easy to implement in practice. However, logistically, this strategy could pose problems. A few pallets must be precooled separately if a container needs to be packed with fruit from the same origin and harvest date, by which the other pallets need to be stored outside or in a cool room for some time. These pallets need then to be again added to the cargo to be shipped, which is not always that straightforward to organize.

3.7. Impact of increasing T-bar floor height on cooling and food quality uniformity within a shipment

3.7.1. Aim

We explore if we can improve the cooling of the pallets and the associated quality preservation by adjusting the height of the T-bar floor that is installed in the containers. To do so, we evaluate 5 T-bar floors with adjusted height, compared to the normal height (H_{tb} = 63.5 mm): 127 mm (2 H_{tb}), 95 mm (1.5 H_{tb}), 79 mm (1.25 H_{tb}), 50 mm (1/1.25 H_{tb}), 42 mm (1/1.5 H_{tb}). Note that in all these simulations, the height of the pallets was kept the same, indicating that the same amount of fruit was transported in each container. A higher T-bar floor can, however, lead to partial blockage of the outlet. We therefore also evaluated a case where the height of the T-bar floor was taken 127 mm (2 H_{tb}), but where the pallet height was decreased with 1 x H_{tb}, by which the outlet was not blocked.

3.7.2. Results

The airspeed, SECT, and RSL are shown in Fig. 19 for two floor heights. Fig. 20 shows the RSL distribution in the fruit pallets for all evaluated floor heights. The average values and standard deviations of the superficial airspeed in the pallets as well as the SECT and RSL, are shown in Table 2. We also quantitatively evaluate the distribution of the SECT and RSL of multiple fruits by placing virtual fruit probes in 58,860 locations in the cargo. This distribution of the SECT and RSL is shown in Fig. 21.

3.7.3. Conclusions

Doubling the T-bar floor height removes the recirculation zone near the refrigeration unit. The airspeed in the pallets and the remaining shelf life gradually decreases towards the door end. The SECT exhibits the opposite trend. These findings are more in line with experimental

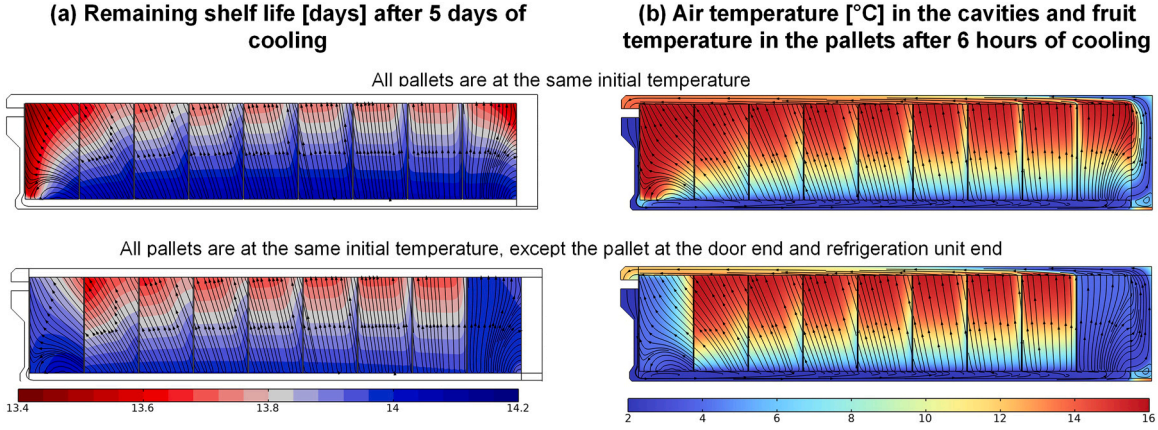

Fig. 17. Remaining shelf life (days) distribution in the fruit pallets after a transport time of 5 days (a) and fruit temperature after 6 h of cooling (b) for non-precooled and partially-precooled cargo.

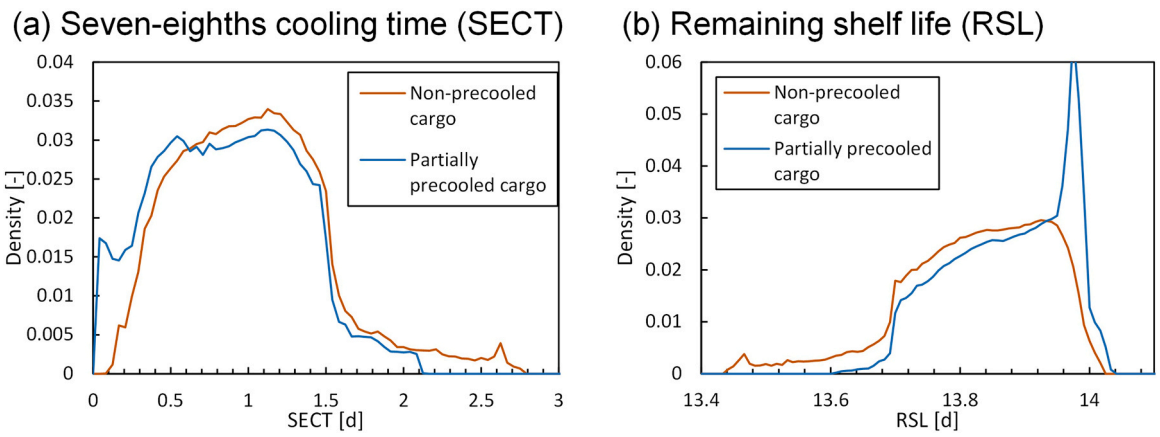

Fig. 18. Distribution of SECT (a) and RSL after 5 days (b) for 58,860 virtual fruit pulp probes inside the cargo for partially-precooled cargo and non-precooled cargo.

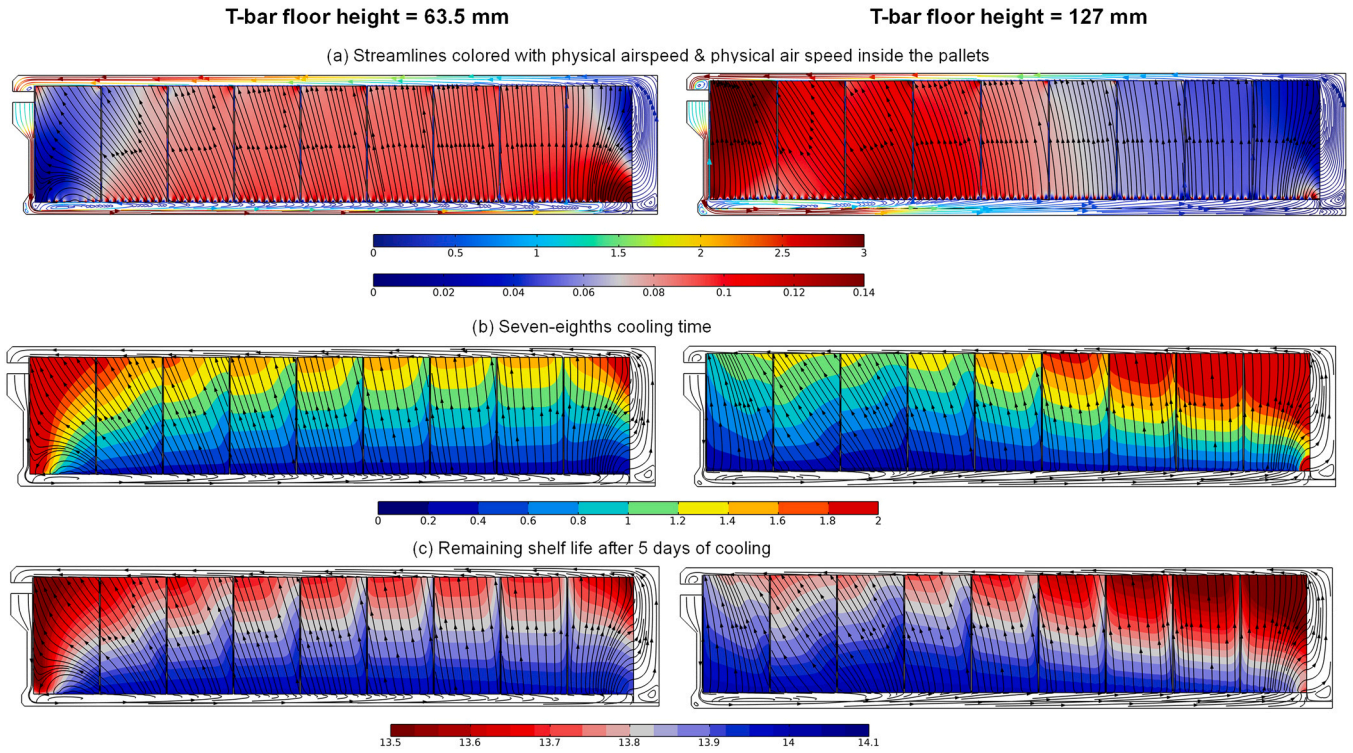

Fig. 19. Physical airspeed (a), seven-eighths cooling time (b), and RSL distribution in the fruit pallets (c) as well as streamlines for different T-bar floor heights.

findings from full-scale experiments and findings from practitioners. They do not seem to find a slow cooling location near the refrigeration unit end. This finding indicates that the turbulence model predictions of the high-speed airflow entering the cargo and remaining attached to the floor by the Coanda effect might not reflect reality for the standard T-bar floor height. However, it is also possible that other packaging and container loading affect the presence of a recirculation zone. More investigation of the possible presence of this recirculation zone is essential in the future (Defraeye et al., 2022). In addition, it is challenging in experiments to achieve the same spatial resolution in cooling and fruit quality evaluation as in the simulations. The averages and distributions obtained by the simulations are, therefore, not exactly comparable to experimental data, which are based on fewer measurement points.

On average, the higher T-bar floor leads to a slower cooling of the pallets and does not preserve quality as well as the lower floor height. The reason is that the pallets near the door end cool slower due to the different airflow conditions. The skewness of the RSL and SECT distributions also increases. However, the pressure drop over the cargo hold is lower with increasing floor height (Table 2). Yet, when the T-bar floor height is doubled, the pressure losses start to increase again, likely due to the partially obstructed outlet. Note, however, that when we would increase the T-bar floor and not increase the pallet height, so if we would remove boxes, this situation could change. This is exactly what is seen for simulation results with the increased height of the floor, but where the pallet height is reduced. We see a more uniform cooling in this case with the lowest SECT of all T-bar floors. Reducing the T-bar floor height leads to a slower cooling, a less optimal quality preservation, and higher pressure losses.

In summary, a higher T-bar floor might remove unwanted airflow zones inside the container, such as the recirculation zone in the pallets near the refrigeration unit end, reducing the pressure losses over the cargo hold. However, the differences in cooling and quality between the pallets at the refrigeration unit end and the door end seem to be

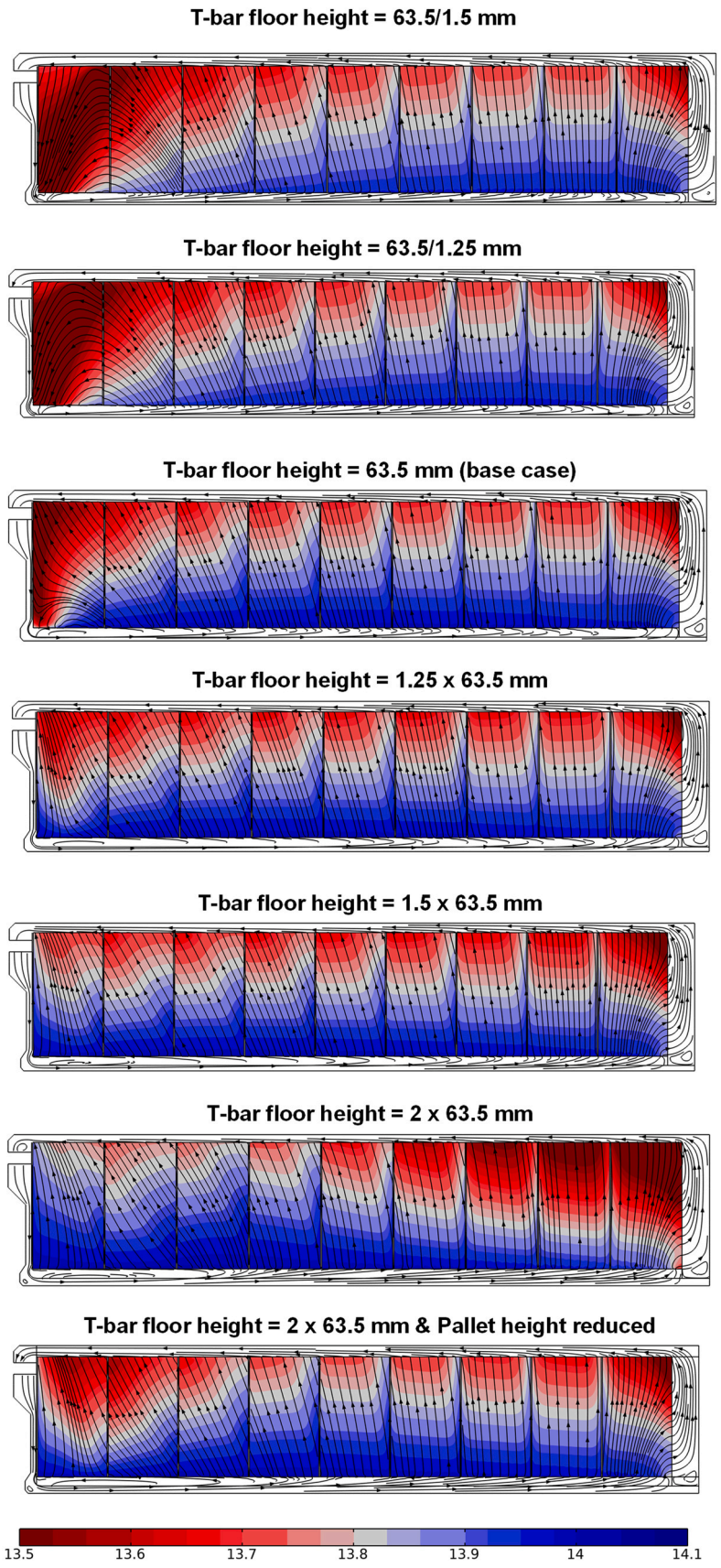

Fig. 20. Remaining shelf life distribution in the fruit pallets and streamlines for different T-bar floor heights.

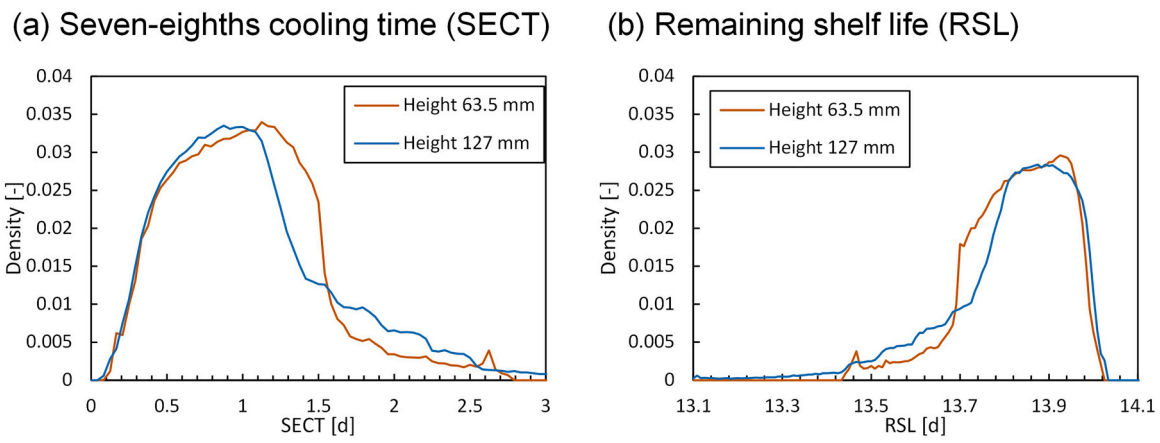

Fig. 21. Distribution of SECT (a) and RSL after 5 days (b) for 58,860 virtual fruit pulp probes inside the cargo for different heights of the T-bar floor.

enlarged. Therefore, these scenarios must be tested more extensively for different loading patterns. Increasing the height of the T-bar floor can be beneficial for cooling and fruit quality preservation. This is however true for high T-bar floors if the outlet section on the top is not obstructed, so if the pallet height is adjusted. This implies that less fruit can be transported per container.

4. Conclusions and outlook

We aimed to gain insight into refrigerated containers' airflow, fruit cooling, and quality preservation. These containers were warm loaded or 'hot stuffed' and cooled down in transit. We obtained this augmented insight by building a physics-based 2D virtual container. We used this model to solve practical questions in refrigerated container transport. Note that the findings of this study, including airflow field and resulting cooling, are sensitive to packaging type and design, the gaps between the pallets, and the loading pattern, among others.

The use of such a 2D model could be justified for this simulation case and has several computational advantages. However, it also has the following limitations, compared to a 3D model: the lateral gaps on the sides of the pallets are not included, the lateral heat exchange of the container with the outside environment is not directly included, the T-bar needed to be included in a simplified way, and the impact of asymmetric stowage patterns cannot be studied. A 3D model would be essential in cases where these aspects play a role.

4.1. Cooling and quality evolution within a refrigerated container

Our simulations captured the main physical trends of container cooling compared with cooling experiments in a refrigerated container, highlighting the reliability of a 2D container model. Especially the vertical gradients are predicted well, where top boxes cooled much slower. The simulations cooled on average 0.3 d faster, so 30%, than the experiments. A particular discrepancy was found in the pallet near the refrigeration unit end. Analysis of the results indicates that the pallets cooled slower in the simulations due to the presence of a simulated recirculation zone. Detailed experiments are needed to elucidate further if this discrepancy is due to the simulations and how the physics-based simulation model should then be improved. Such experiments, where measurements of temperatures and airspeeds are performed at multiple locations inside the cargo, are challenging and resource-intensive.

The airflow in the container is characterized by about 10% airflow bypass via the void at the door end of the container, even with a void plug. The critical locations found for cooling and thermally-driven fruit quality are the fruit at the top of the container and the pallets near the door end and closest to the refrigeration unit. The variation in seven-eighths cooling time within the cargo was over 2 days. The variation in remaining shelf life after the transport period of 24 days was about 0.7 days. As such, not all fruit cool the same, and the quality loss is thus also heterogeneous. A fruit picked by the consumers would last 0.7 days longer when picked from a carton at the bottom of a pallet, compared to the carton at the top at the worst location, due to high-temperature-related fruit quality decay assuming all other aspects are equal at home, given that no chilling injury occurred. In contrast to high-temperature-driven quality loss, the least optimal location for chilling injury incidence or mass loss in the container will be at a different location.

4.2. Different container cooling scenarios

When comparing different scenarios, we found that:

- Cooling at higher airflow rates preserves fruit quality and its uniformity slightly better. We advise that during the container's warm loading or 'hot stuffing', high airflow rates are used for the first three days, after which the airflow can be lowered.
- The positive effect of gaps between pallets on local cooling and ventilation at the pallet edges does not seem to outweigh the negative impact of the resulting cold air bypass. Airflow bypass should be avoided as this leads to less airflow passing through the ventilated packaging. Hence gaps should be avoided for the case considered in this study, namely hot-stuffed, low-respiring fruit.
- A void plug improves fruit cooling rate, uniformity, and quality retention. The type of void plug that is used is less critical since the void plug reduces airflow bypass. Void plug placement is more effective than reducing the small gaps between the pallets.
- By placing precooled pallets at the expected slowest cooling locations in the container, we can mitigate quality problems, for example, at the door end.
- Increasing the T-bar floor height, while keeping the pallet height the same, alters the airflow conditions and hence also the differences in cooling and quality between the pallets at the refrigeration unit versus the door end. Reducing the T-bar floor height is not recommended.

4.3. Outlook

The key merit of the virtual container is that we obtain new, currently unavailable metrics on fruit quality for every single fruit and the heterogeneity within the shipment. We can probe everywhere inside the cargo by placing virtual sensors. In this study, 60,000 probes were used to quantify cooling times and remaining shelf life, for example. These data are currently unavailable in commercial supply chains, or only at one or a few locations or moments in time, as it is too challenging

or resource-intensive to measure them frequently. In contrast to the currently measured single temperature sensor reading in a container, we receive a complete spatiotemporal thermal, fruit quality, and postharvest-life map of all fruit in the container. These in-silico insights enable identifying the pallets and boxes or 'hot spots' that should be prioritized for fruit quality inspection by quality control staff. Also, the best locations to place the sensors by exporters for monitoring the cargo can be unveiled from the simulations. The physics-based model can be extended to other quality attributes (mass loss, chilling injury, pest mortality) and fruits. In that way, ethylene sensitivity and even the partial ripening of the cargo in transit could be studied in-silico, for example, for banana fruit.

This virtual container concept can be extended to cover the entire supply chain from the packhouse to the retail stores. Such a virtual cold chain concept was already put forward but only tested for a single pallet of fruit (Wu et al., 2019b; Wentao Wu et al., 2019; Wu et al., 2018).

However, with this physics-based model, several patterns and correlations in cooling and quality decay remain invisible as these are not included as inputs for the model. Examples are imperfect stacking and packaging of the cargo, fruit cultivar differences, travel delays, the handling practices of different suppliers, human errors in thermal management or logistics, spore presence and resulting microbiological growth, power outages, strikes, or extreme weather conditions (Ndraha et al., 2018; Zhao et al., 2018). In this respect, data-driven initiatives that rely on AI have been developed (Coble et al., 2018; Tiwari et al., 2018; Wolfert et al., 2017), and even commercial platforms are deployed. These data-driven solutions grasp patterns in the sensor and logistics data and thereby complement our physics-based approach, which, in turn, is essential to identify causality and predict the dynamics of food quality evolution. We see that in the future, physics-based model results will be integrated into a data-driven pipeline. Such a hybrid physics-inspired data-driven model would leverage the benefits of both methods.

CRediT authorship contribution statement

T.D. conceptualized the study and acquired funding; T.D. did the project administration; T.D. performed the investigation, developed the methodology, and executed the simulations with key input of C.V. and J. G.; T.D. developed the paper concept and simulations by critical discussions with C.V., J.G., L.L., T.B. and P.C.; T.D. wrote the original draft of the paper; T.D. did the visualization; C.V., J.G., L.L., T.B. and P.C. performed critical review and editing.

Declaration of Generative AI and AI-assisted technologies in the writing process

During the preparation of this work, the authors used Grammarly (full paper) in order to improve the spelling, grammar, and style of the text. No additional original content was generated using these AI-assisted technologies. After using this tool/service, the authors reviewed and edited the content as needed and take full responsibility for the content of the publication.

Declaration of Competing Interest

The authors declare that they have no known competing financial interests or personal relationships that could have appeared to influence the work reported in this paper.

Data Availability

Data will be made available on request.

Acknowledgments

This work was supported by the Swiss National Science Foundation SNSF [200021_169372] and [200020_200629]. The funder was not involved in the study design, collection, analysis, interpretation of data, the writing of this article, or the decision to submit it for publication. We want to acknowledge Michele Ceriotti for sparking the idea of partially loading the container with precooled cargo. We want to thank Richard Lawton from Cambridge Refrigeration Technology for providing us with information on the specifications of refrigerated containers.

Appendix A. Supporting information

Supplementary data associated with this article can be found in the online version at doi:10.1016/j.postharvbio.2023.112722

References

Berry, T.M., Defraeye, T., Nicolaï, B.M., Opara, U.L., 2016. Multiparameter analysis of cooling efficiency of ventilated fruit cartons using CFD: impact of vent hole design and internal packaging. Food Bioprocess Technol. 9 https://doi.org/10.1007/s11947-016-1733-y.

Berry, T.M., Defraeye, T., Wu, W., Sibiya, M.G., North, J., Cronje, P.J.R., 2021. Cooling of ambient-loaded citrus in refrigerated containers: What impacts do packaging and loading temperature have? Biosyst. Eng. 201, 11–22. https://doi.org/10.1016/j.biosystemseng.2020.11.002.

Chaomuang, N., Singphithak, P., Laguerre, O., Suwapanich, R., 2021. Temperature control in a horticultural produce supply chain in Thailand and its influence on product quality. Food Control 118159. https://doi.org/10.1016/j.foodcont.2021.108585.

Coble, K.H., Mishra, A.K., Ferrell, S., Griffin, T., 2018. Big data in agriculture: a challenge for the future. Appl. Econ. Perspect. Policy 40, 79–96. https://doi.org/10.1093/aepp/ppx056.

Defraeye, T., Verboven, P., Nicolai, B., 2013. CFD modelling of flow and scalar exchange of spherical food products: turbulence and boundary-layer modelling. J. Food Eng. 114, 495–504. https://doi.org/10.1016/j.jfoodeng.2012.09.003.

Defraeye, T., Cronjé, P., Verboven, P., Opara, U.L., Nicolai, B., 2015a. Exploring ambient loading of citrus fruit into reefer containers for cooling during marine transport using computational fluid dynamics. Postharvest Biol. Technol. 108, 91–101. https://doi.org/10.1016/j.postharvbio.2015.06.004.

Defraeye, T., Verboven, P., Opara, U.L., Nicolai, B., Cronjé, P., 2015b. Feasibility of ambient loading of citrus fruit into refrigerated containers for cooling during marine transport. Biosyst. Eng. 134, 20–30. https://doi.org/10.1016/j.biosystemseng.2015.03.012.

Defraeye, T., Nicolai, B., Kirkman, W., Moore, S., Niekerk, S.V., Verboven, P., Cronjé, P., 2016a. Integral performance evaluation of the fresh-produce cold chain: a case study for ambient loading of citrus in refrigerated containers. Postharvest Biol. Technol. 112, 1–13. https://doi.org/10.1016/j.postharvbio.2015.09.033.

Defraeye, T., Nicolai, B., Kirkman, W., Moore, S., Niekerk, S.V.S. van, Verboven, P., Cronjé, P., 2016b. Integral performance evaluation of the fresh-produce cold chain: a case study for ambient loading of citrus in refrigerated containers. Postharvest Biol. Technol. 112, 1–13. https://doi.org/10.1016/j.postharvbio.2015.09.033.

Defraeye, T., Tagliavini, G., Wu, W., Prawiranto, K., Schudel, S., Assefa Kerisima, M., Verboven, P., Bühlmann, A., 2019. Digital twins probe into food cooling and biochemical quality changes for reducing losses in refrigerated supply chains. Resour. Conserv. Recycl 149, 778–794. https://doi.org/10.1016/j.resconrec.2019.06.002.

Defraeye, T., Shrivastava, C., Berry, T., Verboven, P., Onwude, D., Schudel, S., Bühlmann, A., Cronje, P., Rossi, R.M., 2021. Digital twins are coming: will we need them in supply chains of fresh horticultural produce? Trends Food Sci. Technol. 109, 245–258. https://doi.org/10.1016/j.tifs.2021.01.025.

Defraeye, T., Lukasse, L., Shrivastava, C., Verreydt, C., Schemminger, J., Cronjé, P., Berry, T.M., Cronje, P., Berry, T.M., 2022. Is there a systematic hidden "hot spot" in refrigerated containers filled with fresh food in ventilated packaging? Trends Food Sci. Technol. 129, 388–396. https://doi.org/10.1016/j.tifs.2022.09.005.

T. Defraeye C. Verreydt J. Gonthier L. Lukasse P. Cronje T.M. Berry Building a physics-based virtual refrigerated container filled with fruit in ventilated packaging engrXiv 2024 doi: 10.31224/3527.

Getahun, S., Ambaw, A., Delele, M., Meyer, C.J., Opara, U.L., 2017. Analysis of airflow and heat transfer inside fruit packed refrigerated shipping container: part I – model development and validation. J. Food Eng. 203, 58–68. https://doi.org/10.1016/j.jfoodeng.2017.02.010.

Geyer, M., Praeger, U., Truppel, I., Scaar, H., Neuwald, D.A., Jedermann, R., Gottschalk, K., 2018. Measuring device for air speed in macroporous media and its application inside apple storage bins. Sensors 18, 1–13. https://doi.org/10.3390/s18020576.

Jedermann, R., Praeger, U., Geyer, M., Lang, W., 2014. Remote quality monitoring in the banana chain. Philos. Trans. A. Math. Phys. Eng. Sci. 372, 20130303. https://doi.org/10.1098/rsta.2013.0303.

Jedermann, R., Praeger, U., Lang, W., 2017. Challenges and opportunities in remote monitoring of perishable products. Food Packag. Shelf Life 14, 18–25. https://doi.org/10.1016/j.fpsl.2017.08.006.

Jiang, T., Xu, N., Luo, B., Deng, L., Wang, S., Gao, Q., Zhang, Y., 2020. Analysis of an internal structure for refrigerated container: improving distribution of cooling capacity. Int. J. Refrig. 113, 228–238. https://doi.org/10.1016/j.ijrefrig.2020.01.023.

Jones, D.A., Clarke, D.B., 2008. Simulation of Flow Past a Sphere using the Fluent Code.

Khumalo, G., Goedhals-Gerber, L.L., Cronje, P., Berry, T., 2021. The non-conformance of in-transit citrus container shipments to cold protocol markets: a systematic literature review. Food Control 125, 107947. https://doi.org/10.1016/j.foodcont.2021.107947.

Merai, M., Duret, S., Derens, E., Leroux, A., Flick, D., Laguerre, O., 2019. Experimental characterization and modelling of refrigeration of pork carcasses during transport under field conditions. Int. J. Refrig. 102, 77–85. https://doi.org/10.1016/j.ijrefrig.2019.02.033.

Mercier, S., Villeneuve, S., Mondor, M., Uysal, I., 2017. Time – temperature management along the food cold chain: a review of recent developments. Compr. Rev. Food Sci. Food Saf. 16, 647–667. https://doi.org/10.1111/1541-4337.12269.

Ndraha, N., Hsiao, H.I., Vlajic, J., Yang, M.F., Lin, H.T.V., 2018. Time-temperature abuse in the food cold chain: review of issues, challenges, and recommendations. Food Control 89, 12–21. https://doi.org/10.1016/j.foodcont.2018.01.027.

Shoji, K., Schudel, S., Onwude, D., Shrivastava, C., Defraeye, T., 2022. Mapping the postharvest life of imported fruits from packhouse to retail stores using physics-based digital twins. Resour. Conserv. Recycl 176, 105914. https://doi.org/10.1016/j.resconrec.2021.105914.

Shrivastava, C., Berry, T., Cronje, P., Schudel, S., Defraeye, T., 2022. Digital twins enable the quantification of the trade-offs in maintaining citrus quality and marketability in the refrigerated supply chain. Nat. Food 1–15. https://doi.org/10.1038/s43016-022-00497-9.

Tiwari, S., Wee, H.M., Daryanto, Y., 2018. Big data analytics in supply chain management between 2010 and 2016: Insights to industries. Comput. Ind. Eng. 115, 319–330. https://doi.org/10.1016/j.cie.2017.11.017.

Wolfert, S., Ge, L., Verdouw, C., Bogaardt, M., 2017. Big data in smart farming – a review. Agric. Syst. 153, 69–80. https://doi.org/10.1016/j.agsy.2017.01.023.

Wu, W., Cronjé, P., Nicolai, B., Verboven, P., Linus Opara, U., Defraeye, T., 2018. Virtual cold chain method to model the postharvest temperature history and quality evolution of fresh fruit – a case study for citrus fruit packed in a single carton. Comput. Electron. Agric. 144, 199–208. https://doi.org/10.1016/j.compag.2017.11.034.

Wu, W., Beretta, C., Cronje, P., Hellweg, S., Defraeye, T., 2019a. Environmental trade-offs in fresh-fruit cold chains by combining virtual cold chains with life cycle assessment, 113586 Appl. Energy 1–11. https://doi.org/10.1016/j.apenergy.2019.113586.

Wu, W., Cronjé, P., Verboven, P., Defraeye, T., 2019b. Unveiling how ventilated packaging design and cold chain scenarios affect the cooling kinetics and fruit quality for each single citrus fruit in an entire pallet. Food Packag. Shelf Life 21, 100369. https://doi.org/10.1016/j.fpsl.2019.100369.

Wu, Wentao, Beretta, C., Cronje, P., Hellweg, S., Defraeye, T., 2019. Environmental trade-offs in fresh-fruit cold chains by combining virtual cold chains with life cycle assessment. Appl. Energy 254, 113586. https://doi.org/10.1016/J.APENERGY.2019.113586.

Zhao, H., Liu, S., Tian, C., Yan, G., Wang, D., 2018. An overview of current status of cold chain in China. Int. J. Refrig. 88, 483–495. https://doi.org/10.1016/j.ijrefrig.2018.02.024.